Chapter 12

Measurement and test techniques

Görgün A. Necati

12.1 Objectives

Objective assessment of vehicle performance necessitates the use of appropriate measuring equipment and testing methods. This chapter describes the instrumentation widely used in vehicle aerodynamics and related vehicle engineering problems. This is followed by a description of testing procedures carried out both in the wind tunnel and on the road.

12.2 Measuring equipment and transducers

12.2.1 Measurement of aerodynamic forces and moments

The precise measurement of the aerodynamic forces and moments acting on a vehicle body is usually done in a wind tunnel. An aerodynamic balance is commonly used to measure the forces and moments. This is a stationary high-precision measuring instrument.

An axis system most widely used is the right-hand orthogonal system (Fig. 4.111). It has its origin at the centroid of the contact points of the wheels with the ground and is fixed in the vehicle. The x-axis is horizontal, pointing forward and in the longitudinal plane of symmetry. The y-axis points to the driver's right and the z-axis points downwards; this is in accordance with SAE Vehicle Dynamics Terminology.[12.1] Confusion may arise if other axis conventions are used and the test results gained with different axis systems are compared by mistake. For example, the axis system commonly in use in flight aerodynamics is shown in Fig. 2.14 and has the x and z axes in the opposite directions.

The axis system used in vehicle aerodynamics has the advantage of coinciding with the axis system commonly used for vehicle handling investigations. This enables wind tunnel data to be used directly with vehicle handling data if the aerodynamic effects on vehicle dynamics are investigated.

12.2.1.1 Wind tunnel balances

A wind tunnel balance measures three aerodynamic force components in the x, y and z directions and three aerodynamic moment components

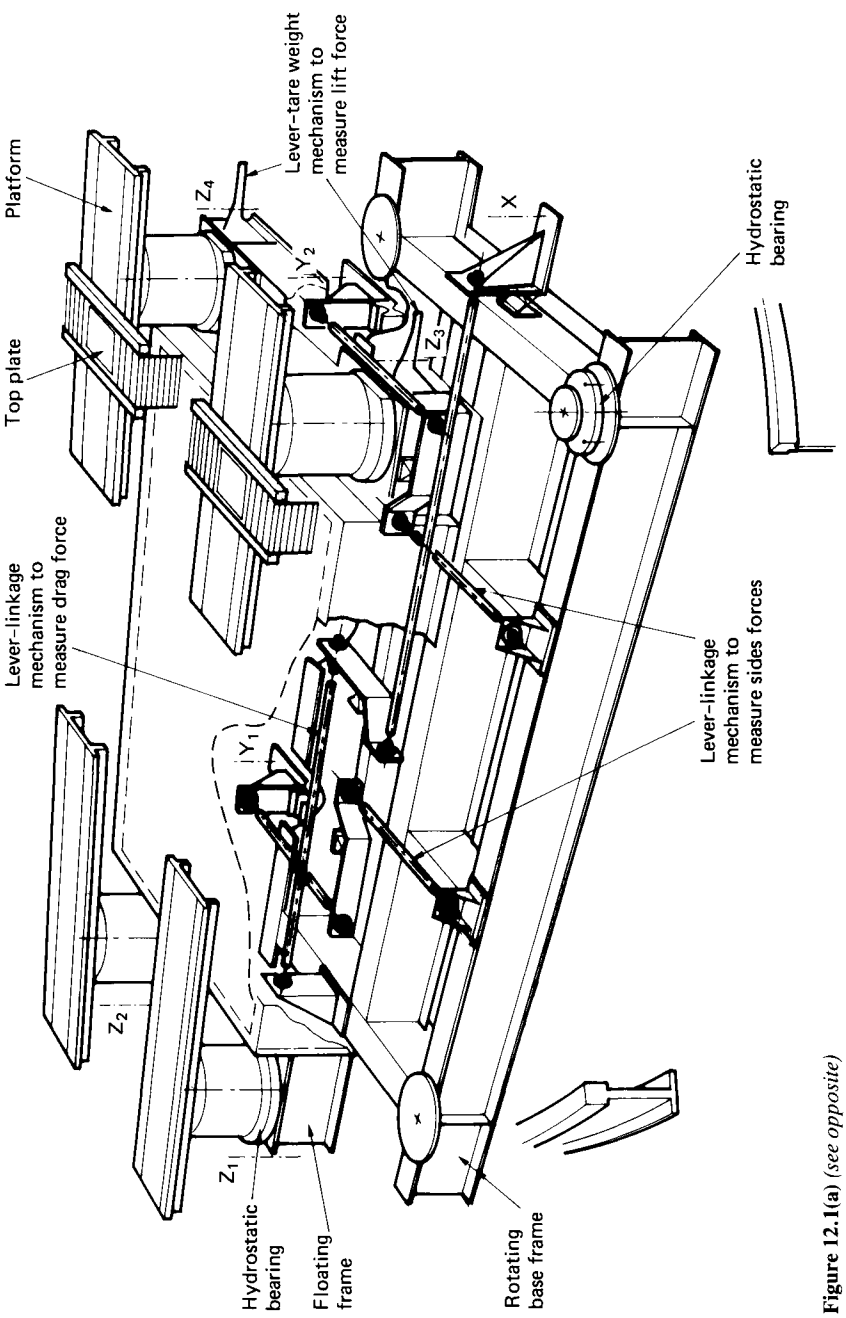

Figure 12.1(a) *(see opposite)*

tending to rotate the vehicle body about the x, y and z axes of the reference axis system. If the aerodynamic yaw angle is zero, the measurement of only three components is sufficient, namely the force components in the x and z directions and the moment about the y-axis. Hence, for tests at 'straight ahead' position only, a balance of simpler design can be used.

To enable precise force and moment measurements to be made, the wind tunnel balances have to satisfy a number of requirements:

- The balance equipment should not disturb the air flow near the test vehicle. If a support system has to be used (e.g. during small-scale wind tunnel tests) the influence of this system on the test results has to be determined for subsequent elimination.
- No changes in vehicle set-up position should occur during the measuring procedure.
- The lift forces to be measured are only fractional compared with the initial wheel loads; hence, for accuracy, tare weights have to be used to compensate the pre-loading in the z direction.
- If the tests are to be carried out at varying yaw angles, provision must be made for the yawing of the balance equipment up to a desired maximum yaw angle.
- Friction and hysteresis must be kept to a minimum in the force transmission mechanisms between the test object and the load sensing systems. The use of special precision components is therefore essential, e.g. knife-edge and groove combinations, elastic hinges, hydrostatic and pneumatic bearings, etc.

12.2.1.2 Resolving the forces and moments into components

The separation method of the three force and three moment components depends on the design of the balance. The six-component balance

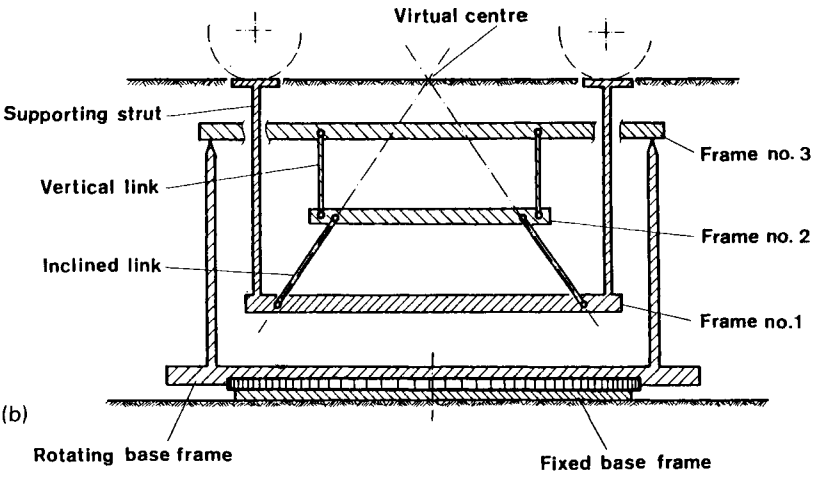

Figure 12.1 Wind tunnel balances. (a) Six-component balance equipped with hydrostatic bearings, base frame and floating frame. The lift force, rolling and pitching moments are calculated from the four lift forces Z_1, Z_2, Z_3 and Z_4. Y_1 and Y_2 enable the side force and yawing moment to be calculated. (b) Working principle and main components of a pyramidal balance

constructions that have been realized for vehicle wind tunnel testing are outlined in the following paragraphs.

One approach to separating the aerodynamic force and moment components is to support the vehicle with four wires parallel to the z-axis, two parallel to the y-axis and one parallel to the x-axis. The force and moment components are then calculated using the measured forces read at all seven wires. This type of force and moment resolution is no longer used in full-scale wind tunnel testing. However, wire type balances are still used in small-scale wind tunnels.

In the second method, the vehicle is positioned on one platform, which is supported on a main frame below the test section by means of three (or four) vertical supports. The horizontal restraint of the platform is provided by three links. The vertical restraint of the platform is provided by three links. The vertical and horizontal supports are connected to load cells to measure the forces transmitted from the vehicle onto the platform. The required vehicle aerodynamic forces and moments can not be immediately read, but are derived from the measured force measurements. This system is applied in the MIRA wind tunnel.

In another construction, each wheel of the test vehicle is positioned on a separate platform, which is instrumented to measure the force components in three directions parallel to the vehicle reference axis system. The resulting aerodynamic force and moment components are then calculated using the 12 signals measured. Such a system is employed in the environmental wind tunnel of Ford-Germany (Cologne), because it is easily removed during environmental tests, when it is replaced by a dynamometer.

Another design often used to separate the aerodynamic force and moment components is shown in Fig. 12.1a. The test vehicle wheels are supported on four platforms, each supplied with a hydrostatic bearing to ensure minimum friction in the vertical direction for immediate lift force measurement. These are mounted on a frame (floating frame) which is supported by four further hydrostatic bearings carried on a second frame (base frame). By means of the hydrostatic bearings, the friction is reduced to a minimum in the horizontal direction. The floating frame is held relative to the base frame in the x-axis direction by means of a linkage lever mechanism to measure the drag force. Two similar mechanisms hold the floating frame in the y-axis direction to measure the side forces. Using all seven force measurements, the required three force and three moment values are calculated. This balance system is most widely used by Volkswagen, Mercedes, Ford (Germany), Fiat, Pininfarina, Saint Cyr (France), and BMW.

The final method has the test vehicle supported on four struts mounted on a frame beneath the test section (see Fig. 12.1b). This frame is attached to a second frame by means of four inclined links (pyramidal balance), as shown. A third frame, which is connected to the second frame via four vertical links, is finally supported by the rotating base frame. The axes of the inclined links have a common intersection point (virtual centre) which coincides with the centre of the vehicle axis system (see Fig. 4.111). As this point is also the moment resolution centre, all three aerodynamic forces and moments can immediately be read on appropriately positioned

linkages without any calculations. The forces in the x and z directions are measured by means of linkage-lever mechanisms which support frame number 2 on the rotating base frame. The force in the y direction is read similarly by means of a double linkage-lever mechanism that supports the second frame on the first frame. For further details on pyramidal balances see Pope and Harper.[12.2] Pyramidal balances are used in the wind tunnels of General Motors and Lockheed Georgia.

Automatic beam balances are often used to measure the forces transmitted from the test vehicle to the force separation system of the wind tunnel balance. This type of balance consists of a weighing beam that has an electrically driven jockey weight. When the beam drops, a driving motor automatically moves the jockey weight in the direction that will balance the beam. The final jockey position represents the magnitude of the force to be measured.

A cheaper way to measure the required forces is to use electrical load cells. These are usually transducers of capacitive or inductive type or strain gauges. However, they need more maintenance than the beam balances and frequent recalibration is necessary.

The upper faces of the platforms on which the vehicle wheels are supported are usually subjected to a decreased static pressure level due to the local air flow regime near the wheels. The static pressure difference between the upper and lower faces of a platform results in an additional force component, which is measured by the balance, and thus to incorrect lift force measurements. The area of the top plates of the platforms must therefore be kept as small as possible. At the same time, provisions have to be made to enable adjustment of the wheelbase and tread width to suit test vehicles of various sizes. Figure 12.1 shows one way of solving this problem. The top plates attached to the platforms can be moved fore and aft to match the desired wheelbase. The remaining areas above the platforms are covered with movable plates supported on the test section floor (not shown in the figure). The lateral position of each of the top plates can also be varied and a belt consisting of a number of slats and supported on the test section floor covers the remaining face. In this way, a flat test section floor is achieved. The top plates, which transmit the forces to be measured to the balance, are isolated from the surrounding turntable by a narrow gap.

Another way of achieving these adjustments is by the use of a system of three eccentric circular plates for each wheel, the smallest being the top plate of balance. The outer two plates are supported by the test section floor. The rotation of these plates allows the desired positioning of the top plate. This enables any combination of tread width and wheelbase to be used. Details are to be found in Kelly et al.[12.23]

If the top plate areas have not been designed sufficiently small, a lift force measurement error is inevitable. In this case, an average static pressure value has to be determined by measuring the static pressure distribution on the upper face of each plate. The difference between the static pressures acting on the upper and lower faces is then multiplied by the plate area to find the lift force component to be taken into consideration as the lift force measurement error.

12.2.2 Pressure measurements

During wind tunnel tests, the most frequent data collected involve the measurement of dynamic or static pressures relative to a free airstream. Measurements are also made of the static pressure distribution created by the air flow over a solid surface.

The measurement of dynamic pressure is usually required to calculate air flow velocity, while static pressure measurement is used to detect the different pressure zones on the vehicle body. These zones are used to determine the air inlet and outlet areas for ventilation and the risk of fume ingress. They are also used to investigate and understand the effects of various aerodynamic proposals (e.g. front end and rear end spoilers) on aerodynamic coefficients.

12.2.2.1 Pressure probes

A common way of measuring the dynamic and static pressure in a free airstream is to use a Pitôt-static tube (Fig. 2.5). The total head g is measured by the orifice at the tip and the static pressure p is measured by the holes or slots in the Pitôt-static tube. If both pressures are connected across a manometer, the pressure difference $g - p$ will represent the dynamic pressure and Eqn 2.11 describes the calculation of free air speed w using the dynamic head (see also Eqn 12.1).

Various types of Pitôt-static tubes are used, the difference being in the head shape. Hemispherical, ellipsoidal and tapered-nose tubes are the most common.

A Pitôt-static tube delivers precise results if it is subjected to a free airstream without large-scale turbulence and swirl. Furthermore, the tube axis must coincide with the air flow direction, otherwise the pressure measurement error rate will vary with the yaw angle. Figure 12.2, from Pope and Harper,[12.2] shows the error versus yaw angle for a Pitôt-static

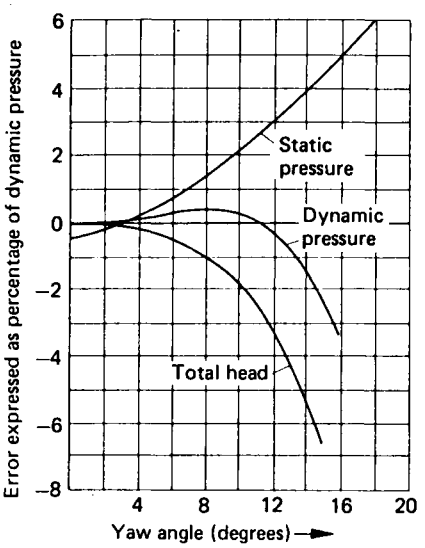

Figure 12.2 Error of a Pitôt-static tube (hemispherical head shape) due to airflow yaw, after ref. 12.2. (*Note*: the static pressure is plotted with negative sign)

tube with a hemispherical head, where up to 12° yaw angle gives less than 1 per cent variation in dynamic pressure which is an acceptable accuracy for most measuring tasks.

The yaw sensitivity of a Pitôt-static tube is strongly influenced by its head shape. The yaw performance of an ellipsoidal nose-type tube, which is also in widespread use, is comparable with the hemispherical head tube. The yaw sensitivity of an N.P.L. tapered-nose standard tube is however considerably higher, as can be seen from Gorlin and Slezinger[12.4] and from Pankhurst and Holder.[12.5] Therefore correct alignment during measurements is particularly essential for this type.

The static pressure distribution on body surface is usually measured by using a small, thin, disk-shaped device, which is sketched at the top of Fig. 12.3a, from Wuest.[12.3] It can be stuck to the vehicle body by means of double-sided adhesive tape. A 0.8 mm diameter hole at the centre of the sensor is connected by means of a radial hole to a tapping soldered on the side of the device and this in turn is connected to a manometer by a plastic tube.

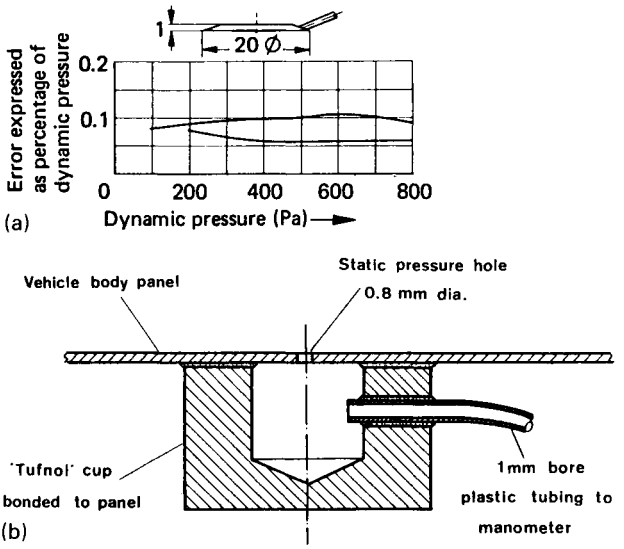

Figure 12.3 (a) Static pressure measuring device and its error after ref. 12.3. (b) Static pressure measurement on body panel without disturbing the local airflow characteristics, after ref. 12.6

Figure 12.3a shows that the error rate of this sensor is negligible if it is used on a flat surface. If the static pressure on a well-rounded surface has to be measured, the error rate of the sensor will however be unacceptably high.

If several sensors are used simultaneously, care should be taken to avoid disturbing the air flow with the plastic tubing, which could result in faulty static pressure results.

Another method of measuring the static pressure on a surface, proposed by Carr and Rose,[12.6] is to drill a 0.8 mm diameter hole in the body panel and to bond a Tufnol cup to the underside. A hole is drilled into the cup

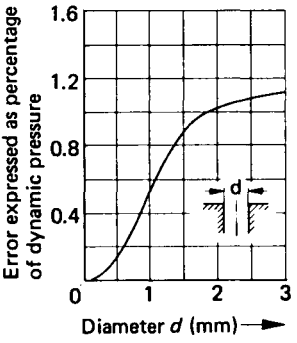

Figure 12.4 Static pressure measurement error caused by the hole diameter of the probe or the hole drilled in the body panel, after ref. 12.4

and a plastic tube is stuck into it to enable the static pressure to be read by a manometer, see Fig. 12.3b.

The incorrect choice of hole diameter may lead to spurious results. Figure 12.4 shows how static pressure error rate depends on the sensor hole diameter. Hole diameters up to 1 mm are considered accurate enough for most measuring applications.

12.2.2.2 Pressure transducers

The pressure probes are usually connected to pressure transducers by a plastic tube. The pressure range in most cases is low (10–1000 Pa) and usually the measurement of differential pressures rather than absolute values is required.

The pressures measured during wind tunnel testing are very seldom steady. Measuring equipment possessing a good damping ability is therefore advantageous. Liquid-column manometers (e.g. U-tube and vertical-tube manometers) are widely used, being uncomplicated instruments with sufficient damping due to the inertia of the liquid column. An inclined-tube version combined with a low density liquid (e.g. alcohol) enables the measurement of the lower pressure ranges.[12.2,12.3,12.5]

The projection manometer (after Betz[12.3,12.5]) is a further development of fluid-column manometers and is fitted with special reading equipment; a magnified image of a floating scale, which moves proportionally to the measured pressure difference, enables pressure readings to be made with a high degree of resolution.

Further commonly used types of pressure transducers are mechanical or electrical types. The mechanical devices use a diaphragm or bellows device to convert the pressure signal to a linear movement and then transfer it to a gauge. With the electrical type, the physical displacement is converted to an electrical signal. Most transducers rely on capacitive, inductive, piezo-electric, potentiometric or strain gauge equipment to generate their signal.[12.4]

The electrical transducers enable continuous data recording on chart recorders or magnetic tape. Moreover, they offer the advantage of computerized data handling, which has advanced sufficiently to make them the most widely used types of pressure transducers.

The mechanical and electrical type pressure transducers exhibit a higher frequency response range than the liquid-column manometers; for most wind tunnel measurements additional damping is therefore required. This can be effected either on the pneumatic side (i.e. between pressure probe and transducer input) or on the electric side (i.e. between transducer output and data recording).

To damp the pressure oscillations and pulsations prior to converting pressure into an electric signal, either resistance or volumetric damping (or both) can be used: the first usually consists of a long plastic tube of small diameter (e.g. 1 mm or less) and the length can be varied to produce the required damping. Volumetric damping is performed by introducing large diameter sections into the connection line between the probe and transducer. The combination of both damping types is advantageous if very small pressure values have to be measured, as for instance during the measurement of air flow through the passenger compartment, see section 12.3.3. If signal damping on the electrical side is preferred, an active filter between the transducer and data recording device enables the desired damping to be obtained.

For certain measuring tasks, the measurement of pressure oscillations and pulsations may be required (e.g. if airflow-induced noise problems are the subject of investigation). In this case, no damping of the pressure signal is desired. The use of a small, highly sensitive pressure transducer located directly at the measuring point without any connecting tubing is effective. Piezo-electric pressure transducers are convenient devices for this type of application.

If the measurement of several pressures in a flow field or the static pressure distribution on a body surface is required, then a pressure scanner combined with one single pressure transducer can be used to measure multiple pressures by 'time-sharing' the single transducer. Test pressures from individual pressure probes are connected to the pressure scanner with plastic tubing and the scanner selects and connects each pressure probe in turn to the pressure transducer. The advantage of using a pressure scanner is the possibility of reading a great number of pressure signals at the lowest cost with only one pressure transducer.

12.2.3 Air flow velocity measurements

The main velocity measurement tasks in a wind tunnel include the determination of wind tunnel operational speed and the air flow speed outside or inside the test car. In some special tests the measurement of the turbulence intensity is also required.

The most common device to measure air flow velocity is the Pitôt-static tube. In the preceding section a method was described of measuring the dynamic pressure of a free airstream using a Pitôt-static tube. From the dynamic pressure, the air flow velocity is calculated as follows:

$$v = \sqrt{\left(\frac{2}{\rho}\Delta p_{\mathrm{dyn}}\right)} \tag{12.1}$$

where v is the air flow velocity in m/s, ρ is the air density in kg/m^3, and Δp_{dyn} is the dynamic pressure in pascals.

The air density varies with temperature, atmospheric pressure and humidity as follows:

$$\rho = \frac{349p_\infty - 131p_e}{T_1} \tag{12.2}$$

where T_1 is the absolute temperature in K, p_∞ is the atmospheric pressure in bar, $p_e = UE/100$ is the partial water vapour pressure in air (bar), U is the relative humidity (%), and E is the saturation vapour pressure at T_1 in bar.

12.2.3.1 Determination of wind tunnel operational speed

A Pitôt-static tube may be used to measure the wind tunnel operational speed by positioning it at the nozzle exit. However, due to the air flow stagnation in front of the test vehicle, the measured wind speed does not correspond to the same wind speed on the road. Hence the wind tunnel operational speed must be calibrated. In doing this, advantage is taken of the fact that above a certain wind speed the static pressure coefficient c_p usually does not vary.

To calibrate the wind tunnel operational speed, one or several cars should first be subjected to road tests to measure the static pressure distribution at several characteristic body areas. The same test procedure must then be repeated in the wind tunnel. From the result of these tests the static pressure coefficient for each body area can be calculated using Eqn 2.9:

$$c_p = \frac{p - p_\infty}{\frac{\rho}{2} V_\infty^2} \tag{12.3}$$

and the graph of the static pressure coefficients from the wind tunnel against those from the road test can be plotted.

As long as the test wind speeds were above the minimum speed at which c_p stays constant, the graphs should be a straight line inclined at 45° and passing through the origin. However, the graph will most likely not be of this form. It may deviate in three ways:

1. The plotted points are scattered from a straight line due to imperfect air flow simulation in the wind tunnel. A first degree polynomial approximation must then be fitted to the curve.
2. The inclination of the fitted line is not 45°. This is caused by the discrepancy between the wind tunnel speed measured with the Pitôt-static tube and the equivalent road speed. From the gradient of the graph, and from the definition of the static pressure coefficient, the correction factor which should be applied to the measured wind tunnel speed V_∞ can be found, according to Carr,[12.7] and thus the wind tunnel operational speed is calibrated.
3. The line does not pass through the origin. This enables the additional information of the relation between the wind tunnel static reference pressure p_∞ and the equivalent atmospheric pressure of the road test to be found. The meaning of this correction has already been discussed in section 12.1.2.2.

The calibration of wind tunnel operational speed with the above method also allows the wind tunnel blockage correction to be taken into account at the same time (see also section 11.3.3).

A further method of calibrating the wind tunnel operational speed is based on measuring the static pressure drop Δp between the nozzle inlet and the nozzle outlet. The dynamic pressure Δp_{dyn} caused by the wind tunnel operational speed V_∞ can be considered proportional to Δp as:

$$\Delta p_{dyn} = \frac{\rho}{2} V_\infty{}^2 = k\Delta p \tag{12.4}$$

which enables the calculation of wind tunnel speed by measuring Δp. The constant k has to be determined from airspeed measurements in the empty test section. This calibration should be performed through the whole speed range of the wind tunnel to check any Reynolds number dependencies. It is recommended that wind tunnel speed calibration be determined by comparing the static pressure distribution on a vehicle body measured on the road and in the wind tunnel, in a similar way to the method described earlier.

12.2.3.2 Measurement of air flow speed outside or inside the test car

The Pitôt-static tube can generally be used for all airspeed measuring tasks if the air flow character in the measuring area is steady and the air flow direction coincides with the axis of the Pitôt-static tube head. The accuracy of this device is, however, not satisfactory at low air flow velocities and if the airspeed is lower than 3 m/s other types of instrumentation are required. Miniature vane-type anemometers are the typical measuring devices used at low speeds.

A vane anemometer consists of a small vane (diameter: 15 mm upwards), mounted coaxially in a cylindrical housing. The rotational speed of the vane is a measure of the wind speed. The operational conditions needed for a correct reading are the same as for the Pitôt-static tube: the air flow mode should be steady and the vane axis has to coincide with the air flow direction. The tolerable yaw until 1 per cent accuracy deterioration is approximately 5 to 7° for an anemometer furnished with a cylindrical housing. This limit can however be increased up to 15 to 20° yaw angle through the aerodynamic optimization of the anemometer housing. On the other hand, special housing shapes have also been developed to read only the wind vector component which coincides with the vane axis up to a certain yaw angle.

The principle behind hot wire anemometers is based on the fact that the heat loss of an electrically heated wire subjected to air flow increases with increasing wind speed. Since the electrical resistance of the wire depends on its temperature, the resistance variation of the exposed wire can be used to measure the air flow velocity. Fig. 12.5 shows schematically the design of a hot-wire anemometer. The wire has a diameter of about 0.005 mm and is welded to two electrodes, which form a fork. The wire is positioned at right angles to the flow direction during the measurements.

One method to determine the air flow velocity is to hold the voltage applied to the wire constant, with the hot wire forming one arm of a

Wheatstone bridge. The bridge unbalances as soon as the electrical resistance of the hot wire changes through air flow application. The amount of bridge imbalance is a measure of air flow speed. This method enables precise measurement of very low air velocities; the measurement sensitivity decreases, however, with increasing air flow speed.

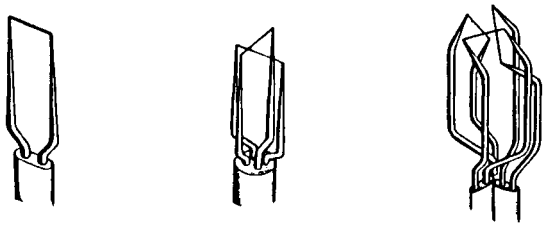

Figure 12.5 Hot wire probes for velocity measurements in one-, two- or three-dimensional flow regimes

A second and more widely used method is constant temperature anemometry: the bridge imbalance due to resistance change of the hot wire is eliminated by changing the electrical current through the sensor with an electronic feedback control circuit. In other words, the temperature of the wire—and consequently its electrical resistance—is held at the same level by changing the current through the sensor. The current change (or voltage change) is a measure of air flow velocity.

In addition to measuring low airspeeds, hot wire sensors are particularly suitable for measuring fluctuating velocities (i.e. turbulence measurements) due to their low inertia. A further advantage is that they can be incorporated in very small probes, which enable measurements to be conducted on rounded body areas or in narrow ducts and gaps without appreciably disturbing the air flow. If multi-sensor type probes are used, two or all three components of the air velocity vector can be measured simultaneously; see Fig. 12.5.

12.2.3.3 Measurement of flow direction

The correct air flow speed measurement in a free air stream requires the air flow direction at the measuring point to be known, so that, as already mentioned, the flow direction sensitivity of the speed measuring equipment can be taken into consideration. The easiest way to position a speed measuring device in the air flow is to detect the flow direction at the concerned area by means of a wool tuft attached to the end of a thin stick.

If the measurement of air flow direction is required to understand or to judge the air flow characteristics in a velocity field (e.g. in the wake of a vehicle), special measuring equipment (yawmeters) can be used for this purpose. The different types of yawmeter for measuring the angular position of the air flow velocity vector in a two- or three-dimensional flow are described in detail in refs 12.3 and 12.4. Two main types of yawmeter are identified: the first group operates on the basis of measuring the pressure difference at symmetrically positioned orifices; the second main type is the hot wire anemometer with multi-sensor probes.

For the pressure difference measurement method, either symmetrically

fitted tubes are used or the differential pressures of orifice pairs positioned on a streamlined symmetrical body are measured. The measurement principle is based on the fact that the pressure difference between two symmetrically positioned tubes or orifices is zero if the flow direction coincides with the symmetry plane of both measuring points. Otherwise a pressure difference is measured, which can be related to the air flow yaw angle through calibration. One pair of tubes or orifices is sufficient for the measurements in a two-dimensional flow. If flow direction measurements in a three-dimensional flow is required, four tubes or orifices are needed, which should be located in pairs in two mutually perpendicular planes. Figure 12.6 shows a spherical yawmeter for three-dimensional flow

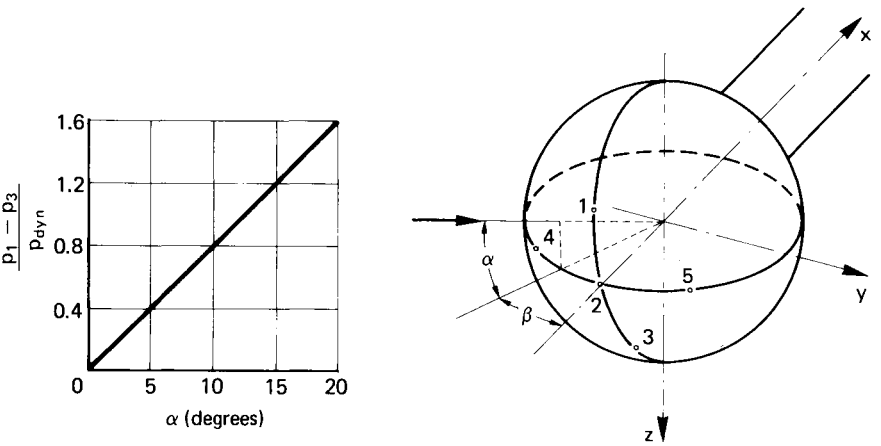

Figure 12.6 Spherical yawmeter and its characteristics (orifice no. 2 for total pressure), after ref. 12.4

direction measurements from ref. 12.4. In addition to the two orifice pairs (nos. 1, 3 and 4, 5) a further orifice (no. 2) at the intersection of the planes serves for measuring the total pressure. If the spherical yawmeter is mounted rigidly in the air flow field, a set of calibration curves is needed for the different combinations of the angular values α and β. However, if the yawmeter is constructed so as to be rotatable about the z-axis, the value of β (in the x-y plane) can first be determined by the null method, i.e. the yawmeter is turned until the pressure difference between points 4 and 5 disappears; the determination of angle α can now be done with the aid of only one calibration curve, as shown in Fig. 12.6.

Flow direction measurements using multi-sensor hot wire probes are done by using specially designed probes consisting of two (or three) mutually perpendicular sensors for use in a two (or three) dimensional flow field. In reality, all two (or three) mutually perpendicular components of the required airspeed vector are measured so that the flow direction and the resulting wind speed can be read simultaneously (see Fig. 12.5).

12.2.4 Temperature measurement

Along with the measurement of air flow characteristics, temperature measurements are often required during wind tunnel tests on a vehicle.

These measurements aim to meet one of the two following objectives:

1. Tests to define vehicle systems performance. The systems mainly concerned are engine cooling, engine starting and fuelling, air conditioning, passenger compartment heating, and defrosting and demisting.
2. Tests to investigate the temperatures of vehicle components. These include all vehicle parts—especially plastics—that may be damaged if subjected to high temperatures, and all vehicle parts which could cause human injury. The brakes, the exhaust pipe, body areas close to the exhaust system, and components in the engine compartment are the most critical parts.

Two different temperature values may be required:

(a) Temperature level at a single measuring point.
(b) Temperature difference between two measuring points.

The first type usually covers most test requirements. If, however, an energy balance has to be established during a performance test, it is necessary to measure the temperature difference of the air or coolant with greater accuracy.

12.2.4.1 Temperature sensors

(a) *Thermocouples*

Thermocouples are the most common temperature sensors used for vehicle wind tunnel testing. Figure 12.7 shows schematically the electrical circuit for a typical thermocouple probe.

A thermocouple is a pair of wires, made of dissimilar metallic conductors, connected (e.g. welded) at both ends. When the two junctions are subjected to different temperatures, an electrical potential is set up between them (also termed electromotive force, EMF), which is approximately proportional to the temperature difference. A voltmeter in the circuit (see Fig. 12.7) can thus measure the temperature difference. If one of the junction points is maintained at a standard reference temperature (e.g. 0°C) the second junction point can be used to measure the absolute temperature at a desired location.

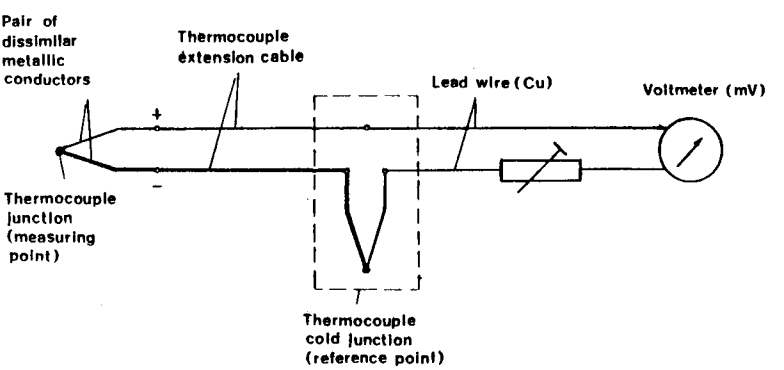

Figure 12.7 Temperature measurement using a thermocouple

The reference junction (also termed the cold junction) can be replaced by an electrical compensation circuit so that the equipment for accurately maintaining a reference temperature can be removed.

The most commonly used thermocouples and their ISA (Instrument Society of America) identification codes are:

Base metal thermocouples	*ISA Type*
Copper–Constantan	T
Iron–Constantan	J
Chromel–Alumel (Equivalent to Nickelchrom–Nickel)	K
Noble-metal thermocouples	
Platinum—10 per cent Rhodium Platinum	S

Keeping the reference temperature at 0°C, the EMF values to be expected at different temperatures are standardized. Table 12.1 shows some EMF figures defined by three different national standards.

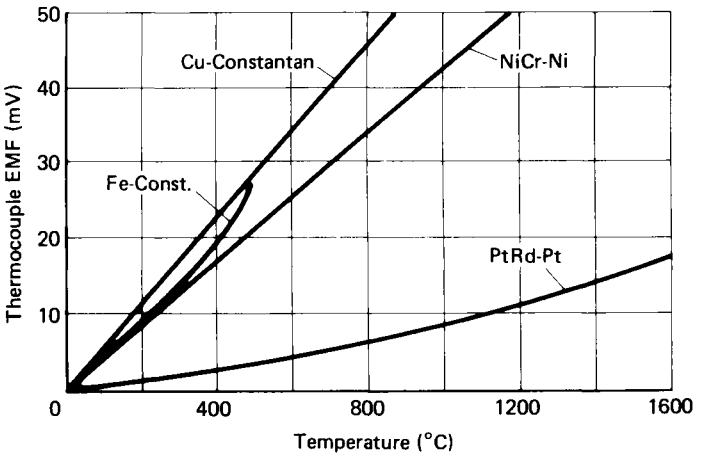

Figure 12.8 Characteristics of different thermocouples (cold junction maintained at constant temperature of 0°C)

Figure 12.8 compares the thermocouple characteristics of the thermocouple types. Iron-constantan and copper-constantan thermocouples are preferred in the temperature ranges of −200°C to +500°C and 700°C respectively. Both these thermocouples produce high EMFs but they tend to oxidize at high temperatures. Chromel-alumel (equivalent to nickel-chrom-nickel) thermocouples can be used beyond 1000°C, and are resistant to oxidation. They exhibit an almost linear characteristic and produce high EMF values. They are therefore very suitable devices for wind tunnel use.

The measured temperature may deviate from the true temperature due to the production tolerances of the thermocouple. The deviation limits for each type of thermocouple are also defined in the national standards. The tolerance band for chromel-alumel type thermocouples is shown in Fig. 12.9. The tolerance bands for noble metal thermocouples are smaller than for base metal thermocouples.

Table 12.1 Review of some standard EMF values of thermocouples defined in German, American and British standards

Temperature (°C)	*EMF* (mV)											
	Copper–Constantan			*Iron–Constantan*			*Chromel–Alumel*			*Platinum–10% Rh–Platinum*		
	DIN 43710	ASTM E 230-72	BS 4937	DIN 43710	ASTM E 230-72	BS 493	DIN 43710	ASTM E 230-72	BS 4937	DIN 43710	ASTM E 230-72	BS 4937
−100	−3.40	−3.378		−4.75	−4.632							
0	0	0	0	0	0	0	0	0	0	0	0	0
100	4.25	4.277	4.227	5.37	5.268	5.268	4.095	4.095	4.095	0.645	0.645	0.645
500	27.41			27.85	27.388	27.388	20.640	20.640	20.640	4.234	4.234	4.234
1000							41.269	41.269	41.269	9.585	9.585	9.585
1500										15.576	15.576	15.576

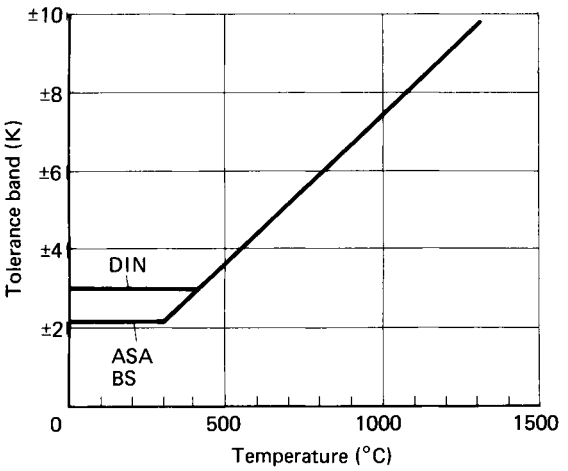

Figure 12.9 Tolerance band for chromel-alumel (or nickelchrom-nickel) thermocouples, as defined by different national standards

(b) *Resistance temperature sensors*

Resistance temperature sensors are usually used during wind tunnel tests if a higher accuracy is required than can be achieved with a thermocouple. The measuring principle is based upon the change of electrical resistance of metals and semiconductors with temperature. The measurement of resistance change will therefore represent the desired temperature measurement.

There is an almost linear relationship between the change in resistance of metals and temperature change (see Fig. 12.10). Semiconductors, however, usually show a non-linear relation and their resistance may either increase or decrease if temperature is increased. They are therefore termed

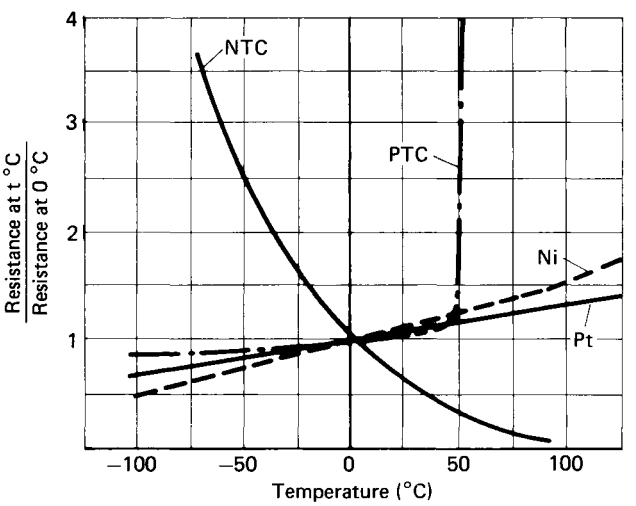

Figure 12.10 Change of electrical resistance of various materials appropriate for use as resistance temperature probes

NTC (negative temperature coefficient) or thermistor (thermal sensitive resistor) probes if a decreasing curve is observed, and PTC (positive temperature coefficient) probes if the resistance increases with temperature.

The change of resistance versus temperature curves of two commonly used metals, platinum and nickel, are given in Fig. 12.10. Very precise temperature measurements in the temperature range of −200°C to +750°C can be made by using platinum of high purity. In practice, the nominal resistance of the platinum sensors at 0°C is usually defined and this resistance is often also used for identifying the probe, e.g. Pt 100 or Pt 500 for probes with nominal resistance values of 100 or 500 ohms at 0°C. As with thermocouples, platinum and nickel resistance temperature sensors are also standardized and their characteristic data are defined in national and international standards. The resistance of the probes at different temperatures and the ratio of the probe resistance at 100°C to the resistance at 0°C (R_{100}/R_0) are compiled. The standards also include information about the tolerances of the probes. Table 12.2 gives an extract

Table 12.2 Extract of characteristic data for Pt 100 defined in the German and international standards

	Platinum		*Nickel*
Temperature (°C)	DIN 43760 (ohms)	ISO (ohms)	DIN 43760 (ohms)
−100	60.20	59.65	
0	100.00	100.00	100.0
100	138.50	139.10	161.8
500	280.93	283.80	
1000		438.2	
R_{100}/R_0	1.385	1.391	1.617

from the standardized characteristic data for platinum and nickel probes with a nominal resistance of 100 ohms at 0°C and Fig. 12.11 illustrates the error range for a Pt 100.

The sensor resistance changes can be measured by including the sensor in a voltage divider circuit or in a Wheatstone bridge. The measurement error caused by self-heating of the sensor due to the current flowing through it (approx. 10 mA) is usually negligible.

12.2.4.2 Typical temperature measurement errors

Temperature measurement may appear to be very uncomplicated, but through bad handling and by disregarding the rules considerable measurement errors may arise. During measurement heat transfer between the sensor and the object usually occurs, and this may result in intolerable errors in temperature readings. Heat transfer by conduction takes place if the surface or material temperature of a solid object has to be measured.

During temperature measurements of a fluid or a gas, heat transfer between the medium and the sensor is by convection. If a high-

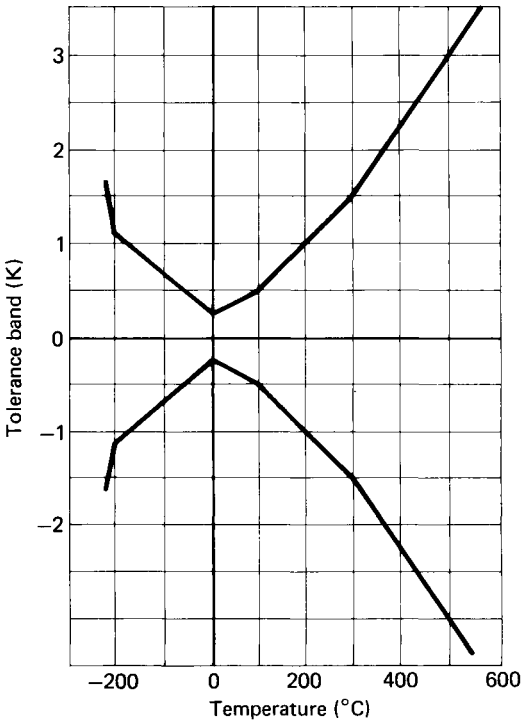

Figure 12.11 Tolerance band for platinum resistance thermometer—Pt 100 (DIN 43 760)

temperature device is located close enough to the sensor, a measurement error due to the radiation from the hot object will occur.

The error due to conduction or convection will be high if a high temperature gradient exists through the sensor and its connection cable. As an example, the surface temperature measurement on a solid object using a thermocouple is shown in Fig. 12.12a, after Lindorf and Marchevka:[12.8] due to heat transfer (conduction) through the sensor the

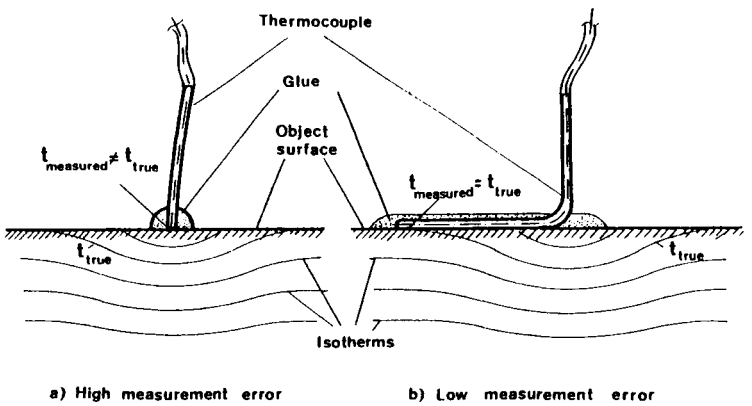

Figure 12.12 Error due to the heat transfer between test object and thermocouple during a surface temperature measurement, after ref. 12.8

isotherms of the object are distorted. Consequently, the temperature monitored by the thermocouple differs from the true surface temperature.

The error increases with a lower thermal conductivity coefficient of the object, higher thermal conductivity and convective heat transfer coefficients (with reference to air) of the sensor, and poorer contact between the sensor and the object. Any or all of these unfavourable conditions may occur if surface temperatures of plastic or rubber devices are measured. Figure 12.12b demonstrates how this error can be eliminated. If a certain length of the tip (and cable) is glued on the surface, the thermocouple junction point, which actually measures the temperature, is thus still subjected to the true surface temperature; the longer the glued piece, the lower the error. Figure 12.13 shows an example of how the error changes with the glued length of a thermocouple. Figure 12.13 also demonstrates the deterioration in accuracy with increasing thermocouple diameter since the thermal conduction of the sensor increases.

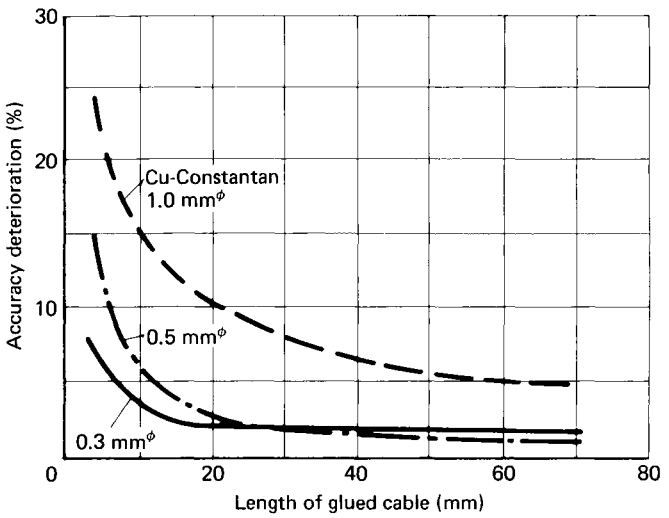

Figure 12.13 Variation of temperature measurement accuracy with glued cable length on the surface and cable diameter, after ref. 12.8

No major alteration in the performance of the test object should be allowed while taking measures to increase temperature measurement accuracy. If for example the thermocouple cable is glued on a surface, the convective heat transfer coefficient of the cable and glue should be comparable with that of the test object. This is important if the test object is small.

If the temperature in a solid object has to be measured, similar means as described for surface temperature measurements should be used to minimize any disturbance of the initial isotherms of the test object.

During temperature measurements of air (e.g. in ducts, etc.) or a fluid (e.g. coolant in hoses, engine oil, etc.) care should be taken to avoid the temperature sensors touching the boundary walls. Furthermore, if a temperature probe is mounted on a wall or on a hose by using fittings,

precautions should be taken to minimize the heat losses through the fittings and thermocouple leads to ensure a true measurement.

Incomprehensible temperature values from thermocouples are usually caused by using wrong thermocouple leads and extension cables or wrong polarity.

Thermocouple material characteristics may change due to oxidation or other chemical influences. Further change in the calibration of thermocouples is caused by ageing, which may result in drifting of several degrees Kelvin per year.

Most of the errors occurring with resistance temperature sensors are caused by faulty insulation of the probe.

12.3 Wind tunnel testing methods

12.3.1 Measurement of aerodynamic coefficients

The aerodynamic forces and moments are measured in a wind tunnel using a wind tunnel balance. The various types of wind tunnel balance are discussed in section 12.2.1. The aerodynamic force and moment figures obtained are then used to calculate the aerodynamic force and moment coefficients as described in section 2.3.3.5.

At the start of the test, the vehicle is set up on the balance top plates and fixed, preferably by locking its driven wheels. High standards of wind tunnel air flow quality are important for obtaining reliable aerodynamic data, but attention should also be paid to some simple test details for good test results.

One important point is the correct loading of the test vehicle to its test weight. Not only the total weight must be checked but also its distribution between front and rear axles. If this is not correct, the riding heights at front and rear will be incorrect and the angle of attack of the vehicle body will not be representative of the intended test case. As the aerodynamic coefficients vary with angle of attack (see section 4.5.2) the test results will be incorrect.

As a result of the lift force components at front and rear axles, the effective axle loads decrease with consequent changes of the front and rear riding heights. However, with independent wheel suspension, the bounce or rebound motions cause simultaneous tread width changes. But, because the wheels are not rotating in the wind tunnel, no tread width change can occur. This results in reduced vertical body movements and therefore to riding heights which do not completely correspond to driving conditions. Measures have therefore to be taken to enable the vehicle tread to change freely during wind application. The easiest way to achieve this is to apply steering wheel motions by a 'driver' prior to every data reading. Thus the riding heights at vehicle front end are truly adjusted. A similar compensation at the rear end is not easy, and as the error is generally small compared with the front end, it can be neglected.

As a result of flow separations and vortices at various points, the vehicle body is subjected to pulsation and the test signals are consequently not steady. The test data reading should therefore be made for long enough to

gain a representative mean value of the parameters measured. The minimum measuring time has to be determined experimentally and is also dependent on the force sensing system of the aerodynamic balance. If the measuring system contains weigh beams instead of electrical load cells, the reading time can be kept shorter due to the higher inertia and thus to the higher damping ability of these devices.

12.3.2 Air flow management tests

Optimization of the air flow characteristics at certain points on the body may be required to develop the performance of various vehicle systems. For this purpose, the flow characteristics around these areas must be identified in order to enable any modifications to be done.

To improve the engine heat rejection through the radiator, the air flow velocity through the radiator core should be increased as much as possible. As has been outlined in sections 4.3.2.12 and 9.3.1, this can be achieved with body front end modifications or by varying the radiator position. To judge the effectiveness of the tested variations, the velocity distribution over the radiator has to be measured. The air flow velocity through the core cannot, however, be easily measured. The reason for this is that the air flow undergoes a swirling motion between grill and radiator. Most anemometers can only measure air flow in the direction for which they have been set up. The continuously changing direction of air flow around the radiator makes the use of these anemometers questionable (see also section 12.2.3.2). If the measurement is carried out at the rear of the radiator, similar measuring difficulties occur due to turbulence caused by the fan. One possibility however is to use hot wire anemometers, suitable for measurements in three-dimensional flow regimes (see Fig. 12.5). These sensors make it possible to determine the air velocity component normal to the core. Moreover, due to their small dimensions, positioning close to the radiator is possible without disturbing the prevailing air flow characteristics. By moving the sensor with a traversing device, continuous tracings of the air velocity distribution across the radiator core can be recorded (see Fig. 9.19).

Another air flow measurement task is the optimization of the brake cooling air flow. A qualitative evaluation of the air flow characteristics can be done by using a smoke generator. A mirror positioned beneath the brake assembly enables the observation of the air flow patterns to be made easily. Furthermore, the air velocity distribution in the area in question can be measured using a hot wire anemometer.

A brake cooling performance test, however, delivers quicker information if the wind tunnel is equipped with a dynamometer facility capable of applying a motoring torque; see section 6.6.2. Using the dynamometer, braking is applied at a representative driving speed (e.g. 100 km/h; 62.5 mile/h) to heat up the brake system. Typical temperatures (e.g. brake fluid, brake disc or drum) are measured. After reading a temperature level representative of severe braking on the road, the brake force is released and the braking system is subjected to tunnel wind until all components have cooled down. The time needed to achieve a selected lower temperature level can be taken as a representative figure to assess the

effective cooling capability of the brake assembly. The effectiveness of different measures to improve brake cooling performance can be investigated by performing successive cooling tests.

12.3.3 Measurement of air flow rate through the passenger compartment

The volumetric rate of air passing through the passenger compartment has to be measured to judge the ventilation performance of the vehicle. Air flow rate measurements are also required for some thermal tests (e.g. passenger compartment heating) to enable the establishment of an energy balance.

The air flow passing through the vehicle interior usually enters the passenger compartment at the cowl inlet and leaves through the extraction openings and leaks in the seals around doors, windows and rear boot lid. The air flow rate is a function of the wind speed V_∞, the yaw angle, and the position of the ventilation/heater flaps and blower speed.

12.3.3.1 Air flow rate measurement by means of 'extraction curves'

This method is often used in vehicle wind tunnel testing (see also section 10.4.1) and consists of two steps:

- establishment of 'extraction curves';
- determination of air flow rate using these curves.

To establish the extraction curves, the air inlet at the cowl has first to be sealed (e.g. by using adhesive tape). The air input into the passenger compartment will now be achieved externally by using an air blower (see Fig. 12.14a). The blower outlet is connected to the car interior by a flexible hose.

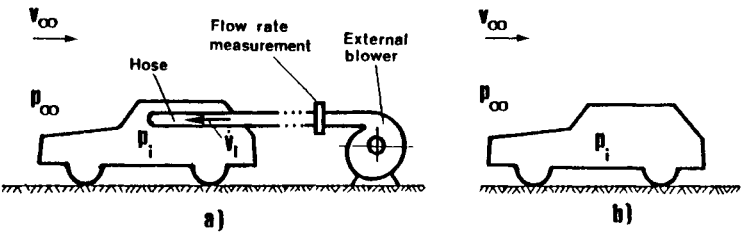

Figure 12.14 Wind tunnel test to measure the air flow rate through the passenger compartment: (a) arrangement to establish the 'extraction curves'; (b) airflow test

The air flow rate is variable and is measured at the air blower exit using an appropriate flowmeter. Measures have to be taken so that the air pumped by the blower flows into the vehicle interior without leaks. The easiest way is to prepare a plywood plate with the contours of a window and then mount and seal it into the opened window. A cylindrical connection piece fitted to a hole in the wooden plate facilitates the connection and sealing of the hose coming from the blower.

To establish the extraction curves, the air flow rate of the blower is changed and the air flow rate $\dot{V}$ and the static pressure increase

$\Delta p_i = p_i - p_\infty$ at the vehicle interior are measured simultaneously. The pressure difference to be measured is usually low; attention should therefore be paid to positioning the measuring point in the passenger compartment at a place where no error can occur due to local dynamic pressure.

The test is first done without wind and then repeated at different windspeeds. All the curves obtained are plotted on a graph as shown on Fig. 12.15. These curves are termed 'extraction curves' of the test vehicle body.

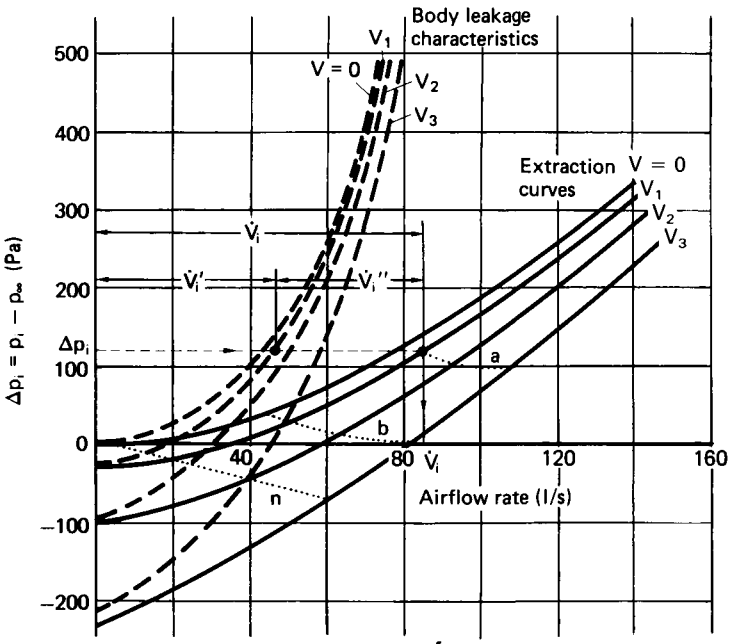

Figure 12.15 Determination of the air flow rate $\dot{V}$ by measurement of the interior static pressure increase Δp_i

Each extraction curve shows the rate of air flow extraction against interior pressure, where the only deviation from real driving conditions is the replacement of the real air intake system by an external air blower. In other words, if the external blower is removed and the air inlet is again opened, the air flow rate occurring under driving conditions can now be determined by using the extraction curves, knowing the wind speed and then measuring merely the vehicle interior pressure.

The above method can be extended to define the amount of air extraction occurring through body leakages. For this purpose the test with the external blower has to be repeated, but with the body air extraction ducts also closed. The remaining air openings are the body leakages and the established curves at various wind speeds show the proportion of the extraction air flowing through the body leaks (see Fig. 12.15).

Once the extraction and body leakage characteristics have been established, the test vehicle is returned to its original conditions by re-opening the air inlet and extraction ducts and removing the external air

supply device (Fig. 12.14b). The required operational position of the heating/ventilation system can now be defined through various flap positions and blower speeds. After setting up the system to a desired position, the vehicle interior pressure is measured at the wind speeds already used to establish the extraction curves, and these points are marked on each corresponding extraction curve, see Fig. 12.15. For each pressure measurement Δp_i and windspeed combination a corresponding air flow rate $\dot{V}_i$ can now be read on the x-axis. Extending all marked points to a curve, a graph is obtained characterizing the performance of the selected heating/ventilation system in the selected operational position. Finally, to show the results more clearly, a further graph can be drawn of the determined air flow rate $\dot{V}$ versus windspeed V, see Fig. 12.16. To give an example, three different operating positions are shown on the graph: curve n indicates the ram air condition while curves a and b show the blower operation at high and low speeds respectively.

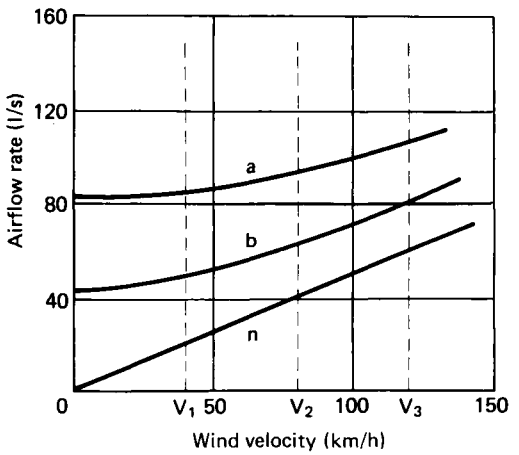

Figure 12.16 Final presentation of airflow rate test results derived from Fig. 12.15

Plotting the test results for all the required operating positions of the heating/ventilation system on a graph as shown in Fig. 12.16 is very informative and enables a rapid assessment of the heating/ventilation system.

A further application of the graph illustrated in Fig. 12.15 is to find out which portion of the measured air flow rate flows through the body extraction ducts and which share flows through the body leakages. If the interior pressure Δp_i at the wind speed V_1 is measured, a horizontal line at Δp_i is drawn and the intersection points of this line with the body leakage and extraction curves are marked (see Fig. 12.15). The total air flow rate $\dot{V}_i$ is divided into two components $\dot{V}_i'$ and $\dot{V}_i''$ at the intersection point with the body leakage curve, where $\dot{V}_i'$ is the air flow share flowing through the leaks and $\dot{V}_i''$ is the share of the extraction ducts.

The body leakage is the result of many small openings. According to Eck[12.10] an 'equivalent leakage cross-section' can however be defined to express the leakages with one single figure (see also section 10.4.1). Using

the body leakage characteristic curve without wind application ($V = 0$) and reading the flow rate V for a selected vehicle interior pressure level Δp_i the equivalent leakage cross-section A_e is defined as

$$A_e = \frac{\dot{V}}{\sqrt{(2\Delta p/\rho)}} \tag{12.5}$$

where all of the leakage openings are assumed to be replaced by one single opening with cross-section A_e. It is usually of interest to check the value of A_e at different Δp_i levels. An 'equivalent cross-section for body extraction ducts' can also be defined, which enables the engineer to assess the effectiveness of the ducts.

The method described is easily carried out and is therefore widely used. It is, however, of limited accuracy due to the assumption that the air intake into the vehicle interior occurs exclusively through the air intake ducts in the cowl and that air exits at every body leak. Consequently, if air intake instead of air exit occurs at some leaks the method will give incorrect results. This situation may occur if the flaps of the vehicle heating/ventilation system are positioned to allow very low air flow rate by ram air while the test car is subjected to wind.

Alternative test methods using different measurement principles can be applied to measure the air flow rate through the vehicle interior, where this shortcoming is eliminated.

12.3.3.2 Alternative methods of measuring the air flow rate through the passenger compartment

A vehicle interior heating test using the vehicle heating system enables the calculation of the air flow rate through the passenger compartment by establishing an energy balance for the heated air passing through the vehicle interior.[12.11] A very good knowledge of the heat loss characteristics at every body area and precise temperature measurements are required to obtain precise test results. This method is therefore impractical.

Another method of air flow rate measurement is to insert a defined volume of an isotope gas (e.g. Krypton 85) as a tracer into the vehicle interior and to measure the concentration while the vehicle is subjected to wind.[12.11] The concentration measurements enable the calculation of the exact ventilation rate through the passenger compartment. CO_2 may also be used as a tracer, which has the advantage that the special precautions necessary for an isotopic tracer are not needed.

Finally, it should be noted that the air flow rate measurement tasks in the wind tunnel are usually performed at a straight ahead position of the test vehicle. The results, however, may change considerably if the test car is yawed to the wind direction, which would correspond to natural cross-wind effects on the road.

12.3.4 Passenger compartment heating and air conditioning tests

A temperature-controlled wind tunnel equipped with an adjustable chassis dynamometer is an ideal facility to conduct passenger compartment heating or air conditioning tests. Because the dimensions of the

temperature-controlled wind tunnels are usually smaller than the aerodynamic wind tunnels (see section 11.5.5), the suitability of the wind tunnel for such tests has to be verified. This validation can be done by examining the correlation between the static pressure distribution on a representative vehicle body measured on the road and in the wind tunnel. This correlation ensures realistic air inlet and outlet rates at body openings and consequently true air flow rates through the heat exchanger of the heating system and through the vehicle interior, which are significant parameters for heating and air conditioning tests.

Figure 12.17 shows a typical recording of a heating test. Prior to the test the test vehicle is usually soaked at the test temperature until all engine and passenger compartment components reach this temperature. The test is then started and the engine is loaded by means of a chassis dynamometer, which for each wind speed is capable of simulating the corresponding tractive resistance. After a predetermined time (e.g. 1 hour) of constant driving, the test speed and corresponding dynamometer drag is increased to a higher level. A third test phase with further increased test speed and engine load follows. During the test the air temperature distribution at several locations in the passenger compartment is recorded. Figure 12.17

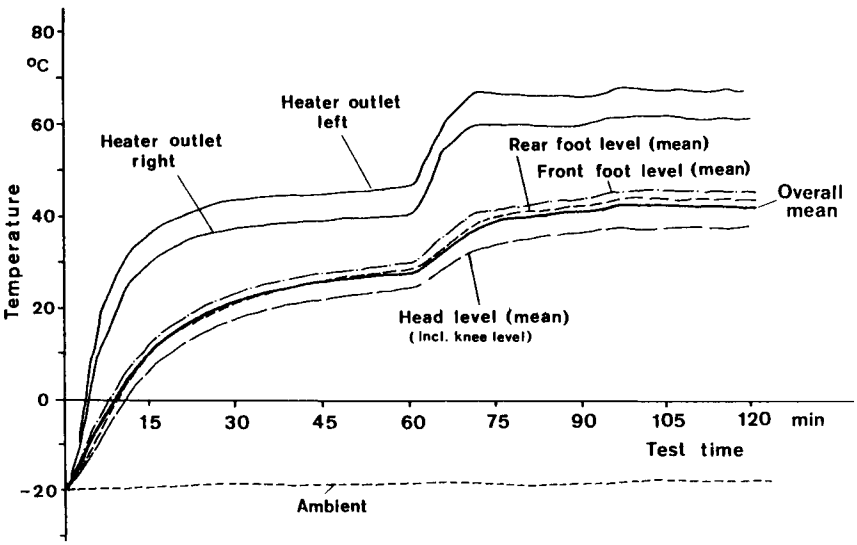

Figure 12.17 Typical vehicle interior heating test recording

shows only the average values of the temperatures at foot, chest and head levels as well as their overall average. The final judgement of the heating system performance is made by comparing the overall average temperature values with 'minimum performance' figures, which are usually set according to practical experience.

The procedure of an air-conditioning system performance test is very similar to the heater performance test: the test vehicle is first soaked at high test temperatures and then the test is carried out with successively increased driving speeds. In addition to the high test temperature level, solar radiant heating by means of special lamps and an increased level of

humidity are applied to simulate the most severe operational conditions for the air-conditioning system. Typical test conditions for an air-conditioning system test are, for example, 40°C or higher, 40 per cent humidity and 1 kW/m^2 solar radiation intensity. The solar simulation lamps should emit parallel rays and possess a spectrum similar to sunlight. Satisfactory correlation with field tests has also been observed if infra-red lamps are used to simulate solar radiation. However, the absorption and reflection of the radiation energy falling on (tinted or clear) glass surfaces are not identical for infra-red and sunlight-similar radiation. Therefore the heating effect on the vehicle interior will also be different and deviations from field test results may be observed.

The evaluation of the air conditioning is done against a minimum performance limit for the average air temperature of the passenger compartment for transient and steady-state behaviour.

12.3.5 Windshield defrosting and demisting tests

Defrosting performance of the heating system is an important requirement for cold climate operation of a vehicle. Several countries require a minimum performance level for windshield defrosting; e.g. FMVSS 103[12.12] is a test standard for North American countries and 78/317/EEC[12.13] is currently being introduced as an acceptance requirement for European countries.

The defrosting test is preceded by a soaking phase until all vehicle components are cooled down to the test temperature. Standard test temperatures are −3°C and −18°C. The test begins with the application of an ice layer on the vehicle glass surfaces of defined thickness (e.g. 0.044 g/cm^2) by spraying water from a spray gun. After the car is soaked for a further 30–40 minutes the engine is started and warmed up, either at a defined idling speed or through driving the vehicle at a partial load. The defrosting system is brought into operation and the defrosted areas of the glass surfaces are marked on their inner faces at five-minute intervals. The defrosting pattern is photographed or traced onto paper on completion of the test. The patterns can be used to assess the performance level of the defrosting system. The judgement of the windshield defrosting capability is especially important and special areas on the windshield are specified in standard test procedures to enable a realistic assessment.[12.12,12.13]

Figure 12.18 shows the defrosted pattern on the windshield. The dotted lines indicate the special areas of the windshield. The minimum performance requirement for a defroster system is established in terms of percentage of defrosted areas in a defined time period for each windshield zone.

During the demisting test, the moisture rejection of passengers (approx. 70 g/h per passenger) is simulated by using a specially designed steam generator.[12.13] The test temperature is slightly below freezing point (e.g. −3°C). After the soaking period, the steam generator is brought into operation for 5 minutes to form a moisture layer on the glass surfaces. The engine is then started and the defrosting/demisting system is put into operation to remove the moisture on the glass surfaces while the steam generator is kept in operation until the test is completed. Patterns of

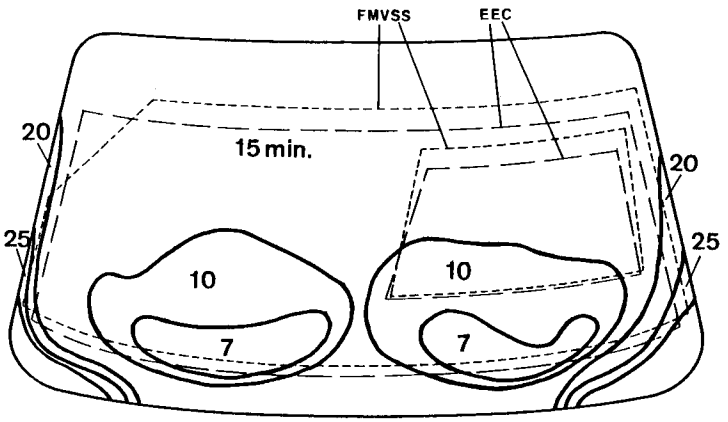

Figure 12.18 Windscreen defrosting test result: patterns show the defrosted windscreen areas at five-minute intervals. The significant windscreen zones are indicated by dotted lines

demisted areas are outlined and documented for evaluation much as for defrosting tests.

12.3.6 Wind tunnel engine cooling tests

The performance of the engine cooling system is usually investigated and developed in a wind tunnel. The tunnel must be equipped with a chassis dynamometer to simulate the vehicle aerodynamic and mechanical resistance. The climbing resistance may also be added if hill climbing simulation is required. The tests are usually carried out at high air temperatures to simulate severe operating conditions. Sun load and tailwind simulations may also be introduced to make the testing conditions even more severe.

A good correlation is observed between engine cooling tests carried out in a wind tunnel and those on the road. As long as the air flow simulation is good at the front end of the vehicle this correlation applies. In other words, reliable cooling test results can be gained in wind tunnels with small nozzle exit areas. Wind tunnel facilities can therefore be designed exclusively for engine cooling tests. Being smaller, they have lower investment and operating costs. Attention should however be paid to the correct calibration of the wind tunnel operational speed since its accurate determination usually becomes more difficult as the nozzle exit area is decreased (see also section 12.2.3.1).

Three main test procedures are applied to check the engine cooling performance in a wind tunnel (see also section 9.2.1):

(a) Simulated top-speed test on level road;
(b) Simulated hill climb test while towing a trailer;
(c) Idling or switch-off of the engine at the completion of (a) or (b).

The dynamometer roll speed and torque can be adjusted to simulate the speed and driving resistance of the test vehicle. The driving resistance must either be computed from test data or read from a traction force-speed diagram, see Fig. 9.4.

The simulated top speed and hill climb tests are continued until the coolant and engine oil temperatures are stable. The most important temperatures to be measured are the radiator coolant in the top and bottom hoses, engine oil and ambient air. For the evaluation of the cooling system, the difference between the radiator top hose coolant temperature t_r and the ambient air temperature t_a is considered to be the most significant parameter as

$$\Delta t = t_r - t_a \tag{12.6}$$

The value of Δt is found to be approximately constant at various ambient temperatures, as long as the thermostat valve opening and the engine fan switch on/off (electric fan) or engagement/disengagement (visco fan) behaviour remain unchanged.

The ambient temperature may be increased up to a limit t_{ATB} where the coolant at the radiator top hose begins to boil. The coolant boiling temperature t_{cb} depends on the cooling system pressure level, which is determined by the opening pressure of the radiator cap.

Extending Eqn 12.6 to the critical boiling case:

$$\Delta t = t_r - t_a = t_{cb} - t_{ATB}$$

hence

$$t_{ATB} = t_{cb} - (t_r - t_a) = (t_{cb} - t_r) + t_a \tag{12.7}$$

t_{ATB} is termed the 'air-to-boil temperature' and represents the ambient air temperature at which the engine coolant would begin to boil if the test car were subjected to similar driving conditions as simulated during the cooling test. The air-to-boil temperature t_{ATB} is therefore considered to be a significant figure in the judgement of the cooling system performance: the higher the air-to-boil temperature, the higher the engine cooling system performance.

It is clear that the engine cooling performance becomes more critical at high ambient temperatures. If the temperature of the wind tunnel is controllable it is better to choose high test temperatures. This is to ensure that the operation of the thermostat and fan is the same as during severe environmental and driving conditions. Otherwise, the air-to-boil temperatures found with relatively low testing temperatures in a wind tunnel may deviate from the corresponding t_{ATB} figures representative of field operating conditions with high ambient temperatures. This problem may, however, be overcome by using a thermostat blocked to its maximum opening and with the fan switch shortcircuited or the fan visco-clutch continuously engaged, whichever is applicable.

If similar operation of the thermostat and engine fan is ensured at two different test temperatures, there is still a minor difference between the air-to-boil temperatures calculated for the two environmental temperature levels. The reasons are the changed volumetric and combustion efficiencies of the engine and the changed density of the cooling air. Using the practical experience gained on various engines, the following correction can be applied to estimate the air-to-boil temperature at other ambient temperatures:

$$t'_{ATB} = t_{ATB} + 0.16(t'_1 - t_1) \tag{12.8}$$

where t_{ATB} is the measured air-to-boil temperature at an ambient temperature of t_1 and t'_{ATB} is the estimated air-to-boil temperature for another ambient air temperature of t'_1.

The air-to-boil temperature of an engine cooling system, calculated after a top speed test, does not necessarily coincide with the air-to-boil temperature established after a hill climb test using the same vehicle. The t_{ATB} figures can therefore be compared only for similar driving conditions.

For each type of cooling test the acceptance level can be defined in terms of air-to-boil temperatures. These limits are based on practical experience. The acceptance limit for top speed tests can be chosen as t_{ATB} = 48 to 55°C, whereas the limit for the hill climb tests may be lower (t_{ATB} = 28 to 35°C). This is because of the lower ambient air temperatures usually prevalent in higher altitude regions. The road gradient for the hill climb tests are usually chosen as 10 to 12 per cent, which corresponds to alpine pass driving conditions.

12.3.7 Flow visualization techniques

Visualization of the flow on the vehicle body, the spatial flow close to the vehicle and the air flow pattern in the passenger compartment is an effective method of investigating and understanding the flow field in and around the vehicle. A survey has been given by Hucho and Janssen[12.14] and by Takagi et al.[11.20] The flow patterns adjacent to the vehicle body surface can easily be made visible by using wool tufts (Figs 6.1, 8.59) and the regions of attached and separated flow can thus be clearly detected. Another method for surface flow visualization is the application of a surface oil film containing coloured or luminescent pigments. Figure 6.2 demonstrates this type of flow visualization. However, attention should be paid to the air flow separation regions because these regions are not always clearly indicated by the oil film method.

The visualization of spatial flow near to the vehicle body helps significantly in understanding and interpreting the aerodynamic effects of interesting body areas and contours. The most widely used tool for this is a smoke generator. Emitting smoke into the air flow enables the flow patterns to be made visible. The smoke generators most widely used are based on heating a mineral oil derivative (e.g. Shell Ondina G17) until evaporation occurs and a dense white inoffensive smoke is provided. The smoke is then injected into the air flow with the aid of a long thin stem. The pictures in the preceding chapters of this book showing flow pattern visualization using smoke filaments demonstrate the widespread use of this technique. A further application of smoke generators is the filling of the separation bubbles and wake zones with smoke to illustrate their form and size (Figs 1.2, 6.3, 6.7, 6.15). In this case the smoke has to be injected directly into the bubble or wake to fill them.

If information about the secondary motion within the separated flow is required, a bubble generator can be used to illustrate the flow patterns within the superimposed flow regimes. Helium-filled soap bubbles are injected into the air flow and their paths are photographed. If the exposure time is well chosen, the superimposed flow patterns can be clearly distinguished on the photograph. This technique is especially suited to flow visualization during small-scale wind tunnel testing, see ref. 12.14.

12.4 Road testing methods

12.4.1 Aerodynamic drag force measurements on freely coasting vehicles

Drag coefficient measurements are usually performed in a wind tunnel. However, test methods have been developed to measure the drag coefficient of a vehicle on the road, though the reliability of these measurements is limited, mainly due to uncontrollable environmental conditions prevailing during the road test. Furthermore, the variability of several parameters causes difficulties and uncertainties during isolation of aerodynamic drag from mechanical drag.

One widely used test method to measure the drag factor on the road is the coast-down test procedure (see Bez[12.15]). The test is performed on a long straight track, which must also be level. Although negligibly low natural windspeed is normally required, Walston et al.[12.16] have described a method to determine the drag factor of a vehicle from a coast down test in a windy environment.

The test vehicle is first brought up to a high speed (if possible close to its top speed) and then is made to coast freely by disengaging the vehicle engine. The vehicle speed change is recorded continuously. The deceleration of the car is caused by the mechanical and aerodynamic drag acting on the vehicle, which can be expressed as follows:

$$m(1 + f)\frac{\mathrm{d}V(t)}{\mathrm{d}t} = D_{\mathrm{M}} + D_{\mathrm{A}} \tag{12.9}$$

where m is the vehicle mass in kg, f is the effective mass increase due to the inertia of rotating vehicle components, $V(t)$ is the vehicle speed in m/s, D_{M} is the mechanical drag including the drag shares of tyres, driveline, bearings etc., in newtons, and D_{A} is the aerodynamic drag in newtons.

f is derived from the equations of motion of the rotating components and is found as

$$f = \frac{\dfrac{I_{\mathrm{d}}}{r_{\mathrm{d}}^2} + \dfrac{I_{\mathrm{o}}}{r_{\mathrm{o}}^2}}{m} \tag{12.10}$$

where I_{d} is the total rotational inertia of the driveline, including the wheels of the driven axle, in $\mathrm{N\,m\,s^2}$, I_{o} is the total rotational inertia of the non-driven axle in $\mathrm{N\,m\,s^2}$, and $r_{\mathrm{d,o}}$ is the dynamic roll radius of the tyres on the driven and non-driven axle respectively, in metres.

The aerodynamic drag is

$$D_{\mathrm{A}} = c_{\mathrm{D}} A \frac{\rho}{2} V^2(t) \tag{12.11}$$

where ρ is the air density in $\mathrm{kg/m^3}$, A is the vehicle projected frontal area in square metres, and c_{D} is the drag coefficient.

Equation 12.9 contains the total drag, which is made up of two different components: mechanical drag and aerodynamic drag. As the deceleration of the vehicle during coast-down is continuously recorded and vehicle effective mass can easily be determined, the sum of both drag forces can be calculated for any desired vehicle speed. The main problem now is the

determination of the mechanical drag, so that the aerodynamic drag can be isolated and the drag factor can be calculated.

One method of determining the mechanical drag is to conduct laboratory tests to measure the dependence on speed of the tyre rolling resistance and the driveline friction torque and then use these to find the total mechanical drag. The confidence level of this procedure is however low, mainly due to the difficulty of accurately measuring the tyre rolling resistance. The common way to measure this is to drive the tyre on the outer (or inner) surface of a drum at the desired speeds. However, a number of test parameters differ from road driving conditions, and therefore the rolling resistance figures obtained on a rig test are usually different from the true road values. The main differences are in the different surface materials of drum and road, the cylindrical driving surface on the drum instead of the flat surface on the road and the difficulty of exact road and ambient air temperature simulation during the drum tests. Furthermore, the additional tyre drag caused by vehicle suspension geometry (i.e. wheel camber, toe-in, toe-out) has also to be estimated.

Another method of determining the mechanical drag is to carry out a road test immediately after the coast-down test where the aerodynamic drag is artificially eliminated. This can be performed by using a 'shrouding trailer', which is a plywood box with no bottom and is large enough to hold the test vehicle; see Carr and Rose,[12.6] and Kessler and Wallis.[12.17] Figure 12.19 illustrates the test set-up.

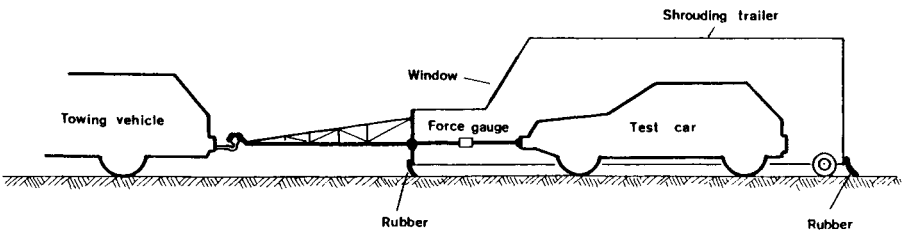

Figure 12.19 Determination of the rolling resistance of a vehicle using a 'shrouding trailer', after refs 12.6 and 12.17

The shrouding trailer is supported by two wheels at the rear and by the trailer hitch of the towing car at the front. The test car is towed by the shrouding trailer by means of a link, instrumented to measure the towing force. The trailer is equipped with a rubber seal around the bottom which is always in contact with the road so that the aerodynamic drag of the test car is eliminated when the combination of shrouding trailer and test vehicle is towed on the road. The force measured on the link between the test vehicle and shrouding trailer is therefore only mechanical drag. This method eliminates all the disadvantages of the previous one, if the measurement of the mechanical drag is performed back-to-back with the coast-down test. However, on the other hand, the driver of the test vehicle has to carry out some steering corrections to stay on course with the towing car, which consequently results in increased mechanical drag. Furthermore, for safety reasons, the combined driving of two vehicles requires the test speed to be limited. This is a disadvantage because at lower driving

speeds the share of the aerodynamic drag within the total drag is smaller, resulting in lower drag factor accuracy.

Several driving speeds are used from the coast-down test in the evaluation of the aerodynamic drag coefficient. The shrouding trailer test has therefore to be repeated at each of the required speeds to determine the corresponding mechanical drag value. The drag factors corresponding to various speeds can then be plotted against vehicle speed to check any Reynolds-number dependencies. To obtain reliable results the whole test procedure should be repeated several times and the results should be averaged.

The above test method enables the determination of the total drag by measuring the vehicle deceleration during a free-coasting manoeuvre. The measurement of total drag can also be done by pushing the test vehicle with another car by means of a link bar, as has been performed by Romani.[12.18] The link bar should be long enough to keep the air flow interference between the vehicles small. The pushing force measured on the bar is equivalent to the total drag. The isolation of the aerodynamic drag has then to be performed as before.

12.4.2 Cross-wind tests

The cross-wind sensitivity of a vehicle can be judged and compared with other vehicles if the vehicle is subjected to an artificially created cross-wind gust during a straight-ahead drive on the road. Figure 12.20 shows

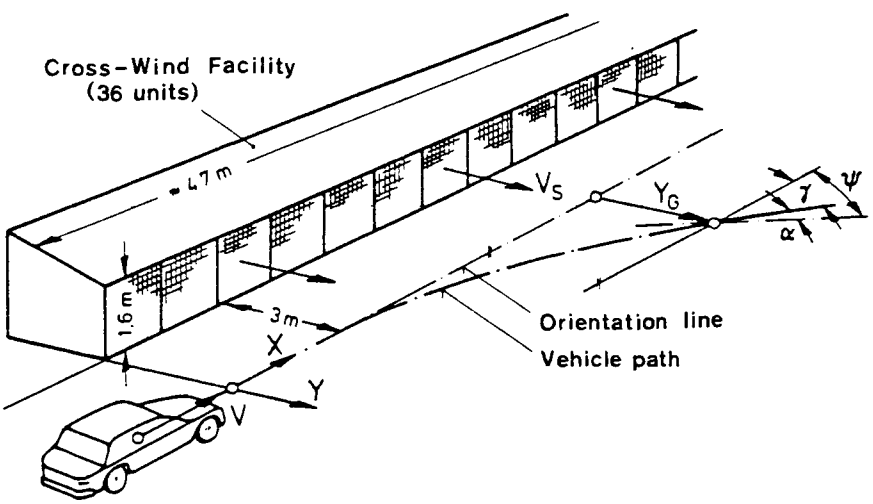

Figure 12.20 Cross-wind test, after ref. 12.20

schematically the performance of a cross-wind test. The lateral deviation of the vehicle from the initial straight-ahead direction is usually considered the most significant parameter in assessing the cross-wind sensitivity of the vehicle.

Cross-wind tests can be performed in two ways (see also section 5.4):

1. The driver does not apply steering correction. The steering wheel of the vehicle is held either constant at its initial position (fixed control) or remains untouched by the driver (free control) throughout the test.
2. The driver attempts to minimize the lateral deviation of the vehicle by steering wheel corrections.

The first method considers only the vehicle response on cross-wind gust and is therefore suitable for comparative tests on one or more vehicles. The second method also includes the driver's response; the test outcomes are therefore primarily influenced by the driver. This method is applied mainly to study driver behaviour or to determine traffic safety performance.

The vehicle lateral deviation can be measured in two ways:

(a) The driver enters the cross-wind gust at a defined point and with zero yaw angle. This is usually done with the help of an 'orientation line', parallel to the battery of the cross-wind generators (see Fig. 12.20). The position of the vehicle during or at the end of the test is defined by markings on the road (e.g. bollards) or sensors under the road surface.

(b) Instrumentation mounted in the test vehicle measures the path curve before and during the test. The equipment to measure the vehicle lateral motion is based on exact measurement of the vehicle lateral acceleration perpendicular to the initial plane of symmetry of the vehicle. Through two successive integrations of the acceleration signal, the lateral deviation of the vehicle is found. Precautions have to be taken to ensure that an exact measurement of the lateral acceleration is made to eliminate the errors caused during the test. This can be done by positioning the accelerometer on a gyroscopically stabilized platform, which maintains the accelerometer in its initial horizontal position in an earth-related coordinate system throughout the test. Finally, the vehicle forward speed has also to be measured for a complete definition of the vehicle path.

Method (a) is quick, easy to carry out and does not need complicated equipment. It is, however, less precise than the second method. One source of error is the difficulty in entering the cross-wind gust with zero yaw angle, due to the steering corrections of the driver immediately beforehand. This error can be allowed for if the gyroscopic instrumentation is used and the test recording is started before the car enters the cross-wind gust.

Although the cross-wind test results enable assessment of the cross-wind sensitivity of a vehicle in general, it is however not possible to derive the aerodynamic coefficients (i.e. side force and yawing moment coefficients) directly from the test results. The reason for this is that the response of a vehicle to a cross-wind gust is affected by two different properties of the vehicle: one is the above mentioned vehicle aerodynamic coefficients and the other is the overall handling characteristics of the car. The significance of the vehicle handling characteristics in cross-wind sensitivity can be demonstrated easily by conducting successive cross-wind tests on a vehicle where the handling behaviour of the car is changed by varying the tyre

Table 12.3 Technical data for various cross-wind facilities[12.19]

	Volkswagen	*Mercedes-Benz*	*Motor Industries Research Association*	*Institute for Road Vehicles, TNO*	*Toyota*	*Nissan Motor Co.*	*Japan Automobile Research Institute*
Cross-wind gust length	47 m	35 m	36 m	11 m	44 m	12 m	15 m
Maximum cross-wind speed	80 km/h	70 km/h	72 km/h	120 km/h	35 km/h 70 km/h	80 km/h	48 km/h 80 km/h 106 km/h
Number of nozzle units	36	16	3	5	15	2	5
Power	VW petrol engines 44 kW each	Electric motors 100–125 kW each	Gas turbine aircraft engine (Rolls-Royce Avon 45 kN thrust)	Petrol engines 147 kW each	Electric motors 95 kW each	V8 petrol engines 132 kW each	Electric motors 320 kW each

pressures of the front and rear wheels. Although the aerodynamic coefficients remain unchanged, the lateral deviation of the vehicle due to cross-wind increases considerably if the vehicle becomes more prone to oversteering (i.e. the tyre pressures of the front wheels are high and of the rear wheels are low).

A number of cross-wind facilities are in operation in different countries. Their characteristic data are outlined in Table 12.3. The comparison shows great differences in gust lengths and wind velocities; consequently only test results obtained in one facility are comparable. Because of the changing wind speed profile and magnitude at different distances to the nozzle units, care should be taken to ensure that the test vehicle always enters the cross-wind test section at a defined distance from the units.

The effective wind velocity vector acting on the vehicle consists of the vehicle driving speed and the cross-wind component. Considerable differences are observed if the effective velocity vector profiles of wind tunnel cross-wind tests and cross-wind facility tests are compared with the profile obtaining during normal road driving. Figure 12.21 illustrates

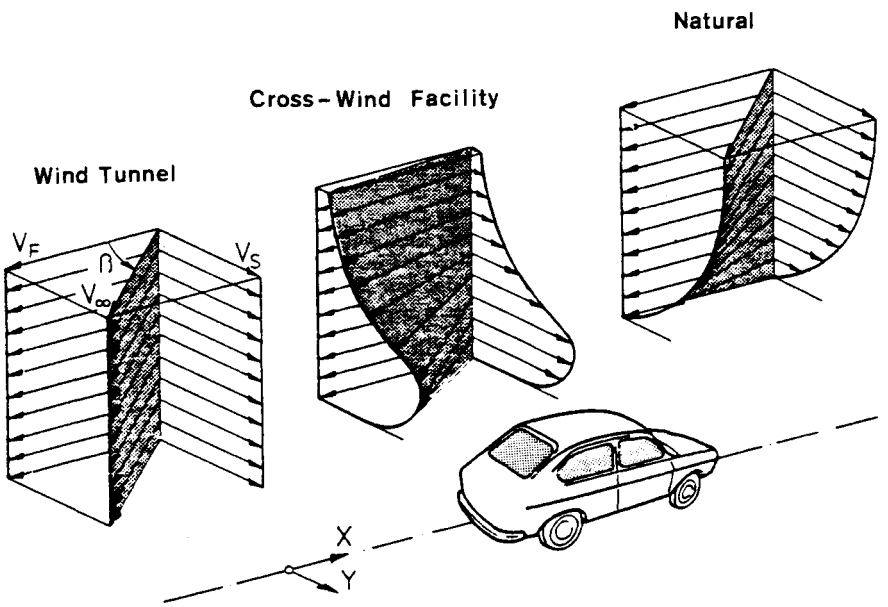

Figure 12.21 Comparison of the effective wind velocity vector profiles prevailing in the wind tunnel, on a cross-wind test track and under natural driving conditions, after ref. 12.20

schematically the differences between the three cases, demonstrating the difficulty in the correlation of cross-wind sensitivity tests with driver assessments under real driving conditions. An actual velocity profile of a cross-wind facility measured at 2 m distance from the nozzles and over a length of 4 m (corresponding to the length of two nozzle units) is illustrated in Fig. 12.22.

If the cross-wind deviations of several vehicles are measured and a ranking is established (see section 5.5), that ranking may change if the test is repeated at another cross-wind or driving speed. The reason for this is

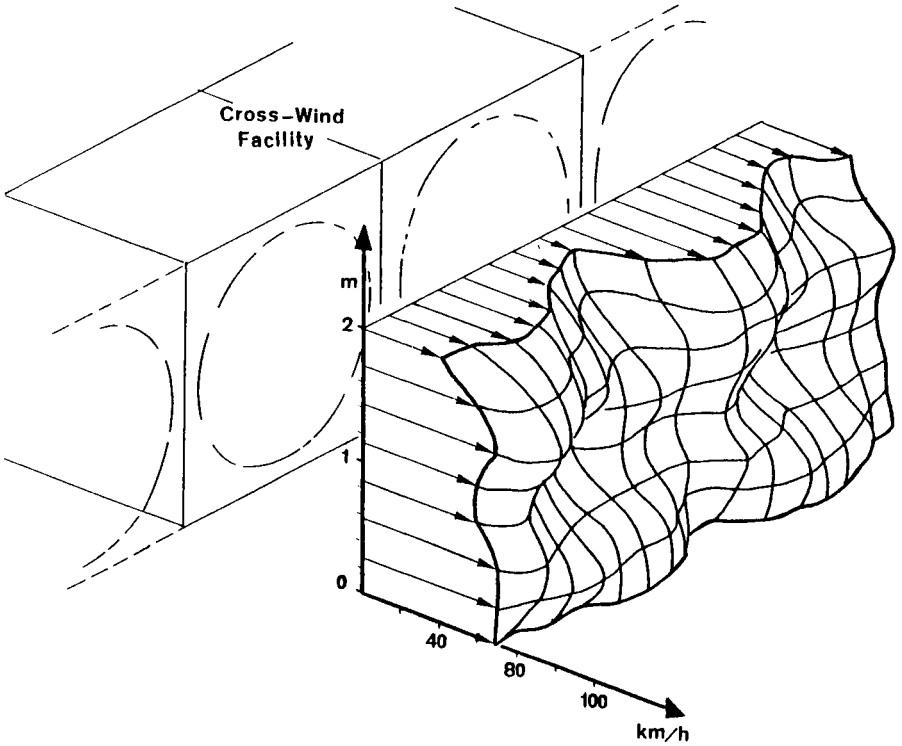

Figure 12.22 Velocity profile of a cross-wind facility

the changed aerodynamic yaw angle β, which results in changes in the side force and yawing moment.

A change in vehicle ranking usually occurs if the test results performed with lower aerodynamic yaw angles (e.g. $\beta = 30°$) are compared with those at extremely high values. However, because accident danger is higher at higher driving speeds, the yaw angle for cross-wind tests should generally be chosen to be less than 30°. Moreover, the maximum of the yawing moment coefficient is usually in this region. In other words, the driving speeds of the vehicle should be high enough to ensure that the test results can be related to real driving conditions.

In the technical literature, methods have been described of investigating vehicle cross-wind response by simulating the road test in a small-scale version (see section 5.2.4). The required parameters of motion are measured as a small-scale vehicle model is moved through a cross-wind gust (see Fig. 5.12). This type of testing is especially useful in the investigation of vehicle transient motion as it enters a cross-wind gust, and so contributes to a better understanding of cross-wind sensitivity problems.

12.4.3 Engine cooling tests on the road

The performance of engine cooling tests in the wind tunnel has already been described in section 12.3.6. Although the same tests can also be carried out on the road, continuously changing environmental conditions

make a systematic investigation and tuning of an engine cooling system impossible. Therefore the road tests are usually performed simply to validate the results gained with wind tunnel testing.

The cooling tests at top speed are usually possible without any major complications if a long level track test or a high-speed loop is available. The performance of hill climbing tests on the road is however not easy, due to the difficulty in finding a test track with a constant gradient, and long enough to enable the engine coolant and oil temperatures to stabilize. This problem can however be overcome by performing a towing test on a level road with a specially designed trailer that can be programmed to dissipate a defined rate of energy during towing. The towing force can thus be adjusted to simulate hill climbing. As with the wind tunnel cooling tests, the results of the road tests are usually presented in terms of air-to-boil temperatures (for definition see section 12.3.6).

The environmental air temperature during road tests changes from one test to another and is often lower than the test temperatures usually chosen in a temperature-controlled wind tunnel. If any comparison between wind tunnel and road test results is intended, attention should be paid to the fact that the air-to-boil temperatures for a given engine cooling system may vary with ambient temperature (see section 12.3.6).

Not all the conditions affecting engine cooling performance are easily simulated in a wind tunnel. One important instance is the effect of altitude while hill-climbing. Due to the decreasing atmospheric pressure and air density at high altitude, the performance and thermal behaviour of the engine change. Therefore it is necessary to correct the cooling system performance by calculating the coolant boil temperature t_{cb} due to the decreased atmospheric pressure. For instance, the pressure at 2500 m altitude is 0.74 bar. An easy simulation of this condition in a wind tunnel is obviously not possible. Therefore the most reliable way to check the engine cooling efficiency in these conditions is to conduct road tests in high altitude regions.

12.4.4 Soil deposits on glass surfaces and body areas

Test methods have been developed for qualitative and quantitative judgement of soil and mud deposits on body and window areas. By performing successive tests, the effectiveness of body contour change can be checked with comparative tests. A reference car can also be used as a basis for comparisons.

In a real driving situation, dirt is deposited on the vehicle by splashing either from the vehicle's own wheels or from other vehicles, see section 8.7. Dirt deposition tests can, in principle, be carried out in a wind tunnel. However, an exact simulation of self-initiated dirt deposition is not possible since the vehicle wheels are not rotating.

A road test method has been described by Hucho[12.20] to investigate the self-initiated soil deposit on a vehicle body. First a test track has to be prepared using a specific soil. The test vehicle body areas under investigation are fitted with small plates. Their weights are measured prior to the test. The test car is then driven on the test track several times. At the end of the test, the plates are removed and weighed again to find the

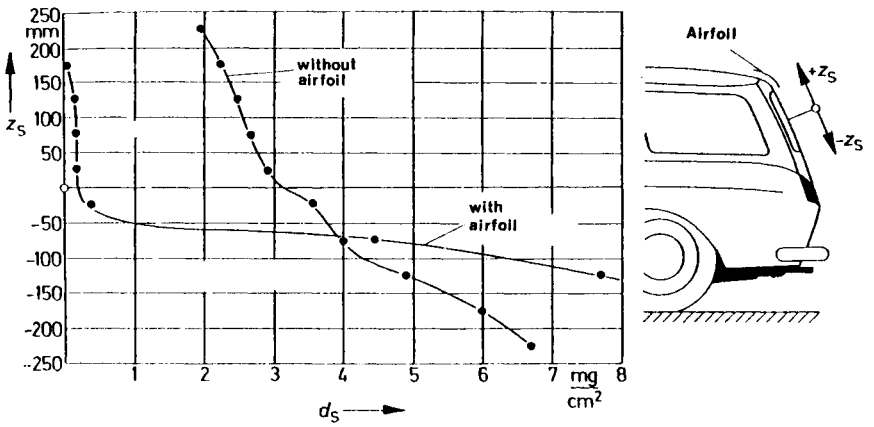

Figure 12.23 Soil deposition test results after driving the test car on a test road covered with dirt, after ref. 12.20

weight increase due to soil deposition. Figure 12.23 shows an example of the test results gained with this test method. The test vehicle, a VW Variant 1600, was tested with and without an aerofoil, as shown on the figure. The results illustrate the ability of the method to highlight the effectiveness of a body modification aiming to decrease dirt deposits on the rear window. The disadvantage of the modification can also be seen: increased soil deposits on the body area beneath the rear window.

An attempt can be made to simulate this test in a wind tunnel by replacing road mud splashed by the wheels with water sprayed at vehicle wheel areas. In this case the small plates used to measure the soil deposits should preferably be covered with thin dry sponge pieces. A further test procedure can be applied in the wind tunnel by spraying water ahead of the test vehicle to investigate the soil deposits caused by dirt thrown up by a preceding car.

Another road test method to investigate soil deposition is to apply a thin layer of oil on the required body areas and then to feed talcum into the airstream in a manner similar to the way the wheels kick up mud or dust from the road surface. The talcum concentrations found on the car surfaces represent the soil deposits to be expected under natural driving conditions. Figure 6.17 shows the test results gained with the talcum method, showing the effectiveness of using an aerofoil to keep the rear window free from dirt.

The talcum method can be applied in a wind tunnel too, but it has the disadvantage that the wind tunnel becomes dirty. This is not only annoying because of the dirt but it may also disturb sensitive wind tunnel instrumentation.

12.4.5 Wind noise measurements

The sources of the wind noise heard in the vehicle interior are mainly the vortices caused by the air flow separations at various body areas. Due to the unsteady character of these vortices, the air in the separation bubbles is subjected to pressure oscillations (see also sections 2.3.4.1 and 6.5.2). If

these are transmitted to the vehicle interior they will be experienced by the passengers as noise. The pressure pulsations may reach the passenger compartment after being more or less attenuated by body materials. Another possibility is a direct link to the vehicle interior due to defective door or window seals or through ventilation openings.

Considerable success has been achieved in the reduction of mechanical and combustion noise in modern cars. It can therefore be very annoying if the wind noise level, which increases rapidly with vehicle speed, is too high. The first step to reduce the wind noise is the isolation of this component out of the total sound level measurement (SLM).

The SLM recordings usually contain the superimposed noise of combustion, mechanical, tyre and wind noise components. Hence direct identification of the wind noise component from a SLM trace recorded during a road test is not possible. One major noise component, the combustion noise, can be eliminated if the engine is switched off at a high driving speed. The mechanical noise is also partially mitigated if the transmission is shifted to neutral. But tyre noise is still present with the wind noise. All noise components except wind noise are eliminated if the vehicle is subjected to airstream in a wind tunnel. However, in this case the wind tunnel noise, which is usually high, is superimposed on the vehicle wind noise.

Although absolute isolation of wind noise is not possible, testing methods have been developed to investigate and reduce wind noise problems. These methods can however only be applied efficiently if the wind noise is the dominant component of a SLM recording. This requirement is met if the SLM difference between the wind noise and remaining noise components is at least 5 to 7 dB. If tested in a wind tunnel, the same SLM difference between wind tunnel noise and wind noise must be attained.

Under certain environmental conditions, a road test can be conducted to check compliance with this requirement. The test is performed on a road where a steady breeze blows with almost constant velocity and direction. Two successive sound level measurements, one with headwind and the other with tailwind, have to be carried out while the engine is switched off and the vehicle coasts. The compliance of the resulting wind speed

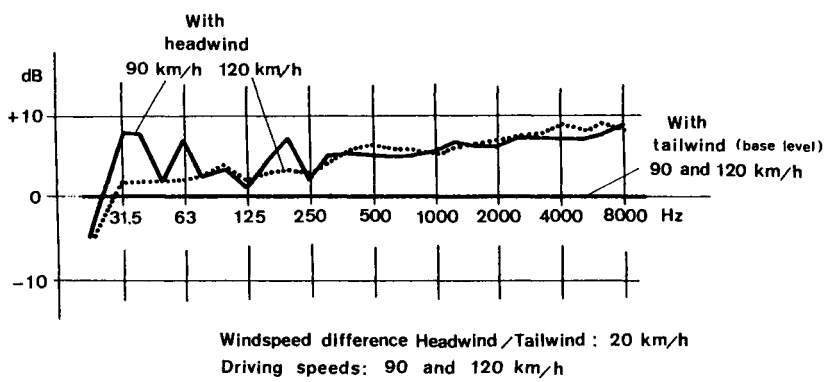

Figure 12.24 Determination of wind noise and tyre noise contributions in road tests, after ref. 12.22

direction with vehicle symmetry plane can be ensured by using an appropriate yawmeter device (see section 12.2.3.3), preferably attached on the roof of the car. Both sound level measurements have to be done at the same road speed. If the recordings are compared, the difference between them is due exclusively to the air flow speed difference of the two tests.

Figure 12.24 shows the SLM difference between two headwind/tailwind tests, one carried out at 90 km/h (56.3 mile/h) and the other at 120 km/h (75 mile/h) on the same vehicle, according to Grosshäuser and Brunkhorst.[12.22] Air flow speed difference between both cases is 20 km/h. The required 5 to 7 dB level variation is not present throughout the whole frequency range. The wind noise is observed to be dominant in the range above 315 Hz. In other words, the efficiency of any measures to reduce the wind noise level can be judged by comparing the SLM patterns in this frequency range.

Another thing that must be known is the maximum achievable wind noise reduction. This is important as it enables the judgement of the improvement that can be achieved with a proposed feature, bearing cost in mind. To find the maximum wind noise reduction level, all the potential wind noise sources have to be eliminated to make a basic SLM recording: for this purpose the windshield wipers and outside mirrors are removed, the drip rail and edges are modified to give smooth edges and all door and hood gaps and ventilation openings are sealed with adhesive tape. The wind noise in a vehicle prepared in this way is barely audible and a noise level measurement performed with this vehicle can be considered as the

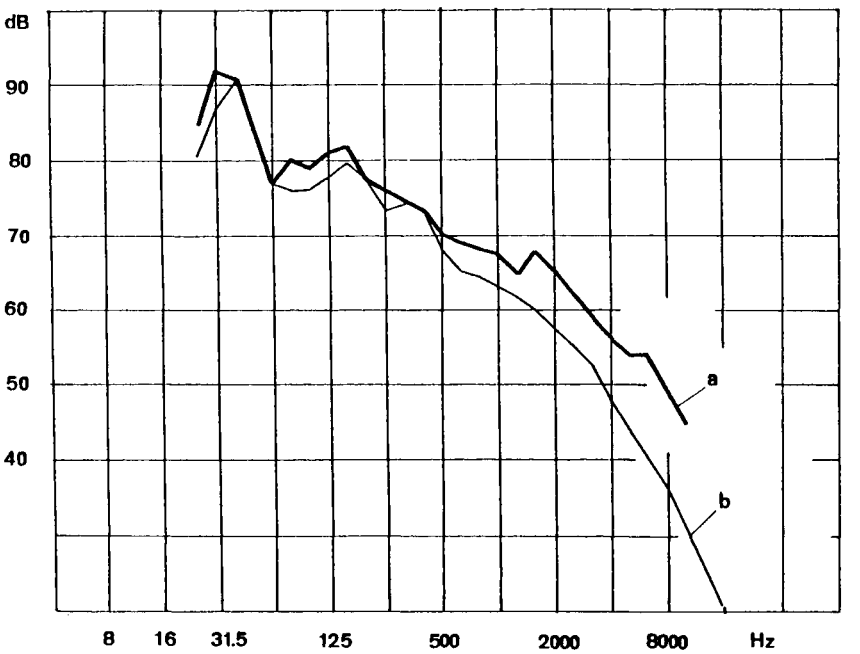

Figure 12.25 Determination of maximum achievable wind noise reduction level, (a) vehicle in initial condition, (b) prepared vehicle, after ref. 12.22

lowest possible level. Figure 12.25 shows the highest achievable noise reduction level compared with the vehicle's initial condition.

The most widely used method of tackling wind noise problems is to take successive sound level measurements on the road or in the wind tunnel. Using the SLM curves, the effectiveness of the proposed body or component detail variations is then compared within the representative frequency range, which has been already ascertained. This enables an objective evaluation of wind noise.

12.5 Notation

A	vehicle projected frontal area (m^2)
A_e	equivalent leakage cross-section (m^2)
D_M	mechanical drag, including the drag shares of tyres, driveline, bearings, etc. (N)
D_A	aerodynamic drag (N)
E	saturation vapour pressure at T_1 (bar)
I_d	total rotational inertia of the driveline, including the wheels of the driven axle ($N\,m\,s^2$)
I_o	total rotational inertia of the non-driven axle ($N\,m\,s^2$)
T_1	absolute temperature (K)
U	relative humidity (%)
$\dot{V}$	airflow rate (l/s)
V	vehicle speed (m/s)
V_∞	wind tunnel operational speed (m/s) (or vehicle driving speed during a road test)
c_D	drag coefficient
c_p	static pressure coefficient
f	effective mass increase due to the inertia of rotating vehicle components
k	wind tunnel speed calibration factor
m	vehicle mass (kg)
p	static pressure (Pa)
p_e	partial water vapour pressure in air (bar)
p_∞	wind tunnel static reference pressure (bar) (or atmospheric pressure during a road test)
$r_{d,o}$	dynamic roll radius of the tyres on the driven and non-driven axle respectively (m)
t	temperature (°C)
t_a	ambient air temperature (°C)
t_{ATB}	air-to-boil temperature (°C)
t_{cb}	boiling temperature of engine coolant (°C)
t_r	radiator top hose coolant temperature (°C)
v	airflow velocity (m/s)
β	aerodynamic yawing angle (degrees)
Δp	static pressure difference between two points (Pa)
Δp_{dyn}	dynamic pressure (Pa)
ρ	air density (kg/m^3)